



2017

PAM-1 Localizations in the Regulation of Autophagy during *Caenorhabditis elegans* Oogenesis

Ashley N. Munie
Murray State University

Follow this and additional works at: <https://digitalcommons.murraystate.edu/steeplechase>



Part of the [Cell Biology Commons](#), and the [Developmental Biology Commons](#)

Recommended Citation

Munie, Ashley N. (2017) "PAM-1 Localizations in the Regulation of Autophagy during *Caenorhabditis elegans* Oogenesis," *Steeplechase: An ORCA Student Journal*: Vol. 1 : Iss. 2 , Article 6.
Available at: <https://digitalcommons.murraystate.edu/steeplechase/vol1/iss2/6>

This Undergraduate Thesis is brought to you for free and open access by the The Office of Research and Creative Activity at Murray State's Digital Commons. It has been accepted for inclusion in Steeplechase: An ORCA Student Journal by an authorized editor of Murray State's Digital Commons. For more information, please contact msu.digitalcommons@murraystate.edu.

PAM-1 Localizations in the Regulation of Autophagy during *Caenorhabditis elegans* Oogenesis

Cover Page Footnote

This work would not have been possible without the support of Dr. Trzepacz, the past and present Worm Lab at Murray State, and the Murray State Biology Department. We would like to thank those that assisted in funding this research, including Kentucky EPSCoR, MSU Committee on Institutional Studies and Research, MSU Office of Research and Creative Activity, and MSU McNair Scholars Program.

Introduction

Autophagy (*self-eating*) describes the process of removing and degrading cytoplasmic components via the lysosome. This can occur in one of the following three ways: through a mechanism of lysosomal engulfing (microautophagy), through chaperone mediated delivery to the lysosome (chaperone-mediated autophagy), or through the formation of an autophagosome around cytoplasmic components and subsequent fusion with the lysosome (macroautophagy, hereafter referred to as autophagy) (Klionsky *et al.*, 2003; Massey *et al.*, 2004). Autophagy was first identified in mammals over fifty years ago when a glucagon-induced response was observed alongside starvation conditions in rats (Deter & De Duve, 1967). In response to glucagon and a variety of other stimuli, cytoplasmic contents are engulfed within autophagosomes and broken down into their respective subunits by enzymes in the lysosome, and are then exported into the cytoplasm and reused by the cell (Yang *et al.*, 2006). Autophagy has since been found to be a highly-conserved process, essential in times of cellular stress such as starvation, hypoxia, or infection in all animals (Abounit *et al.*, 2012). However, this cellular “recycling” process has recently been implicated as a major player in tissue homeostasis, development, aging, and disease (Mizushima & Komatsu, 2011; Choi *et al.*, 2013; Mehrpour *et al.*, 2010).

The genetic regulation of autophagy was studied initially in *Saccharomyces cerevisiae*. Isolation and characterization of the autophagy related genes (Atg genes) was a crucial stepping stone for molecular biologists (Nakatogawa, 2009). In yeast, the autophagic mechanism is primarily used for survival in an environment lacking nutrients (Nakatogawa, 2009). Because of the highly-conserved nature of the autophagic process in eukaryotic organisms, most Atg genes in yeast have orthologues in other model organisms such as in *Mus musculus*, *Drosophila*

melanogaster, and *Caenorhabditis elegans* (Nakatogawa, 2009). Regulators of autophagy have been extensively studied in this variety of model organisms, and findings in higher eukaryotes have implicated autophagy not only as a mechanism of survival during starvation, but also in times of cellular stress, infection, and organelle and protein malfunction (Mizushima, 2007). Autophagy is a ubiquitous process; basal levels of autophagy preserve cell and tissue efficacy (Mizushima, 2007). Mutations in crucial autophagy genes contribute to disease throughout the body, typically in the brain, in the liver, and in the immune system (Mizushima and Komatsu, 2001).

Perhaps the most common disease model of autophagic dysregulation is neurodegenerative disease. The accumulation of cytotoxic protein aggregates causes cellular stress, which leads to cell degeneration or, in other cases, tumorigenesis (Mizushima, 2007). Excessive protein aggregation in the nervous system threatens neuron efficacy, which can be witnessed in cognitive decline, behavioral issues, or movement dysfunction (Choi *et al.*, 2013; Mehrpour *et al.*, 2010). This form of autophagic dysregulation contributes to multiple neurodegenerative diseases, such as Alzheimer disease, Huntington disease, and amyotrophic lateral sclerosis (Mizushima & Komatsu, 2011). For example, in Huntington disease the accumulation of polyglutamine (polyQ) containing proteins are normally degraded via autophagy because of the cytotoxic nature of the fragments created by proteasomal breakdown (Bence *et al.*, 2001). Failure to break down these proteins because of autophagic dysregulation results in their aberrant aggregation and subsequently the symptoms of this disease. In other systems, autophagic dysregulation has been linked to cancer, heart disease, metabolic disease, diabetes, alcoholic hepatitis, Paget's disease, Chronic Obstructive Pulmonary Disease (COPD), and increased pathogen susceptibility (Mizushima & Komatsu, 2011; Choi *et al.*, 2013).

Mechanisms of Autophagy

Autophagy is initiated in yeast by the formation of a pre-autophagosomal structure (PAS), an association of autophagy proteins prior to the growth of the phagophore (*Figure 1*) (Kim *et al.*, 2001; Suzuki *et al.*, 2001; Suzuki & Ohsumi, 2007). The formation of the PAS requires the assembly the PtdIns-3-kinase complex. The PtdIns-3-kinase complex associated with PAS formation in yeast is comprised of Vps30/Atg6, Vps34, Vps15, and Atg14 (Nakatogawa, 2009). Similar proteins exist in higher eukaryotes (Nakatogawa, 2009). Vps30/Atg6, and the mammalian equivalent Beclin-1, is a fundamental part of this complex and has been studied regarding its role mediating the crosstalk between apoptosis and autophagy (Kang *et al.*, 2011). In *C. elegans*, an orthologue of Atg6, *bec-1* has been found to be required for survival, for mutations in the gene cause shortened life span and sterility of the worm (Fazeli *et al.*, 2016; Schiavi *et al.*, 2013). In mammals, a PAS structure has not been identified, but it has been hypothesized that higher eukaryotes have multiple PAS-similar structures (Chen & Klionsky, 2011; Itakura & Mizushima, 2010). While it is known that the PtdIns-3-kinase complex is essential for formation of a phagophore, its exact mechanism of action is unknown (Nakatogawa, 2009).

The PAS is used to nucleate the formation of the phagophore, a dynamic double membranous structure whose origins are currently debated. As the phagophore expands, it envelops pockets of the cytoplasm and unwanted cell contents (*Figure 1*) (Abounit *et al.*, 2012). The yeast autophagy protein Atg8 has been found to be essential for this elongation. Atg8, a ubiquitin-like protein, is conjugated to phosphatidylethanolamine (PE), a phospholipid on the expanding membrane. Atg8 plays an important role in cytoplasm to vacuole targeting by attracting essential proteins, such as aminopeptidase I (ApeI) and α -mannosidase

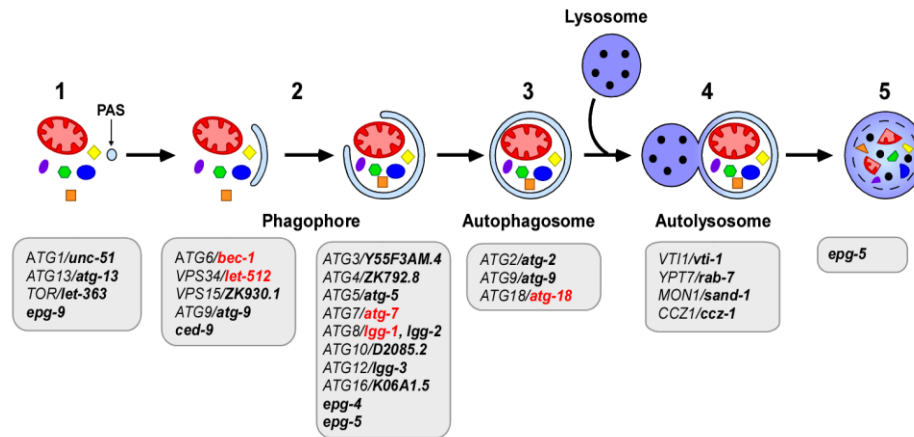


Figure 1: The autophagic process. The diagram above shows the processes of autophagy. The PAS forms (1) and elongates around unwanted cell contents (2), and then fuses to form the autophagosome (3). The autophagosome then fuses with the lysosome to form the autolysosome (4). The cellular contents are degraded and recycled within the cell (5). The yeast autophagy related (Atg) genes are shown beneath the step they regulate. The *C. elegans* orthologues are shown bolded to the right. RNAi suppression of the genes in red were examined in a previous study (Cude and Trzepacz, unpublished).

(Ams1) to the vacuole (Nakatogawa, 2009; Shpika *et al.*, 2011). There is also evidence to support Atg8 acting as a recruiting factor for other Atg proteins to the autophagosome membrane (Shpika *et al.*, 2011). While there is only one Atg8 protein in yeast, in higher eukaryotes there are duplicates whose roles have become more specific and have been further classified into families. For example, *Drosophila* have two genes of the GABARAP family of Atg8 proteins (Shpilka *et al.*, 2009). Humans have two GABARAP family genes, one GATE-16 family gene and four LC3 family genes, one of which has an alternative splicing pattern (Shpilka *et al.*, 2009). *Caenorhabditis elegans* have one GABARAP family gene, *lgg-2*, and one LC3 family gene, *lgg-1* (Shpilka *et al.*, 2011). Each of these orthologues of Atg8 have similar yet distinct roles in their respective organisms to accomplish the task of membrane elongation and recruitment.

After elongation, the phagophore will then enclose to form an autophagosome (Figure 1) (Abounit *et al.*, 2012). Some mammalian autophagosomes will then fuse with endosomes to further mature the vacuole

(Mizushima, 2007). The autophagosomes will then fuse with the lysosome to create the autolysosome, which contains hydrolases that break down the contents inside (Mizushima, 2007). The lysosomal hydrolases will also break down the inner membrane of the autophagosome, including membrane bound proteins such as Atg8 (Mizushima, 2007). The term “autophagic vacuoles” is often used to describe autophagic structures when the specific structure cannot be differentiated. The amino acids produced by the degradation of the unwanted cell contents, the inner membrane, and the membrane proteins are exported and reused in the cytoplasm (Yang & Klionsky, 2009). The contributions of the breakdown of other macromolecules, such as lipids and carbohydrates, to the cell is unknown (Yang & Klionsky, 2009).

There are two different forms of autophagic degradation as seen in the following: degradation to increase nutrient availability in cells and targeted degradation to protect cellular integrity. Each is mediated through its own mechanism. In the case of starvation, autophagy is initiated by nutrient deprivation (Takeshige *et al.*, 1992). In yeast, nitrogen, carbon, or single amino acid deprivation can induce autophagy (Takeshige *et al.*, 1992). Autophagy can be induced in mammalian tissue culture by deprivation of amino acids essential to the cultured tissue (Mortimore & Poso, 1987). In mammalian organisms, the regulation of autophagy cannot be cellularly dependent for maintenance of tissue homeostasis is the main function of the cells. Instead, during nutrient deprivation, organs and tissues, such as the liver, kidney, and adipose tissue, respond appropriately to hormonal signals (Mortimore & Poso, 1987). Cellular autophagy is also stimulated by an abundance of glucagon and is suppressed by the presence of insulin (Mortimore & Poso, 1987). The different exposures and sensitivity of these organs to the hormonal regulators mediates the level of autophagy in the cells. For example, the liver, which is sensitive to hormonal changes, degrades a large amount

of cytoplasmic protein (25-40%) after 48 hours of starvation (Mortimore & Poso, 1987).

The mechanism of hormonal control involves the TOR (target of rapamycin)/phosphatidylinositol 3-kinase (PI3K)/AKT pathway, an essential nutrient regulatory pathway (Lum *et al.*, 2005). When PI3K is stimulated by insulin, the growth factor cytokine Interleukin-3 (IL-3), or insulin-like growth factors, increases external nutrient intake (Lum *et al.*, 2005). The TOR (and the orthologues mTOR in mammals and dTOR in *D. melanogaster*) protein receives input from PI3K through phosphorylation of AKT and is a direct negative effector of autophagy (Lum *et al.*, 2005). In addition to receiving signals from nutrient necessity, TOR also receives signals about nutrient availability, and in this way, can regulate basal levels of autophagy (Tokunaga *et al.*, 2004). When nutrient availability is high, or when growth factors are present, TOR will become active and will activate its downstream targets, which will eventually induce CAP-dependent protein synthesis, a mechanism of translation initiation which relies on a modified 5' guanosine termed a cap (Tokunaga *et al.*, 2004; Lum *et al.*, 2005). The intake of nutrients downplays the need for autophagic action in the cell. These pathways, when inducing the intake of nutrients, also suppress autophagy (Lum *et al.*, 2005). When TOR is inactive, by low levels of insulin or a decrease in nutrient availability, its downstream targets are not active and autophagy is not suppressed. In this way, TOR is a negative effector of autophagic control. It is also important to note that while the inactivation of the TOR pathway may be the most extensively studied mechanism for initiation of autophagy, there are also mechanisms for TOR-independent activation of autophagy (Mordier *et al.*, 2000; Kanazawa *et al.*, 2004; Sarkar *et al.*, 2007).

Induction of targeted autophagy is likely regulated by ubiquitination of the unwanted cytoplasmic content. The polyubiquitin-binding protein p62 can recognize and bind to ubiquitinated proteins targeted for degradation (Komatsu *et*

al., 2007). In this manner, p62 collects in cytosolic protein aggregates (Komatsu *et al.*, 2007; Bjorkoy *et al.*, 2005). p62 interacts directly with Atg8 orthologues on autophagosome membranes to induce the uptake of the cargo and the subsequent degradation (Mizushima & Komatsu, 2011). The autophagic vacuoles involved in p62 binding are initially created through the pathways discussed previously (Mizushima & Komatsu, 2011). There is no known mechanism for initiation of a targeted phagophore.

In selective types of autophagy, specific organelles are targeted for degradation, either because of damage or a severe nutrient deficiency (Nakatogawa, 2016). The mechanism of this selective autophagy is similar to targeted autophagy; receptor proteins on the autophagosome, such as Atg8, recognize signals located on the organelle to be degraded (Okamoto, 2014). One form of selective autophagy is mitophagy, degradation of the mitochondria (Nakatogawa, 2016). Mitophagic dysregulation has direct implications in Parkinson disease (Pickrell & Youle, 2015). Parts of the nucleus and nuclear membrane can also be selectively degraded in a selective autophagic process termed macronucleophagy (henceforth referred to as nucleophagy) (Mochida *et al.*, 2015). Nucleophagy has been observed in yeast under severe nitrogen deprivation (Nakatogawa, 2016). The autophagic receptor protein Atg39 has been implicated in sequestration of the nucleus in this model. It is unknown if nucleophagy in yeast is induced to preserve the integrity of the nucleus under starvation conditions or if it is used to provide the cell with more nutrients in a nutrient depleted environment (Nakatogawa, 2016). In *Tetrahymena thermophile* and some fungi, digestion of entire nuclei occurs proactively during cellular development, but is also used as a reactive mechanism to combat infection (Akematsu *et al.*, 2010; Shoji *et al.*, 2010; He *et al.*, 2012). Nuclear digestion is also observed in wild-type cells in some instances (Park *et al.*, 2009). Disruption of nucleophagy in these cells causes nuclear abnormalities, suggesting a role for nucleophagy in regulation of cellular homeostasis (Park *et al.*, 2009). Although

nucleophagy has been observed in higher eukaryotes, homologues for Atg39 have not been found (Nakatogawa, 2016). The process of nucleophagy in these organisms is believed to be regulated through a different mechanism (Nakatogawa, 2016; Mijaljica & Devenish, 2013).

There are many non-Atg proteins that have been found to regulate autophagy through various of the following mechanisms: AMP-activated protein kinase, an enzyme involved in regulating starvation response (Meley *et al.*, 2006); BNIP3, primarily described as a regulator of cell death (Daido *et al.*, 2004); p19 ARF, a known tumor suppressor (Reef *et al.*, 2006); DRAM, a damage related autophagy modulator and a target of p53 (Crichton *et al.*, 2006); TRAIL, an inducer of apoptosis (Mills *et al.*, 2004); FADD, a modulator of apoptosis with roles in regulating cell proliferation (Pyo *et al.*, 2005; Thorburn *et al.*, 2005); and the Puromycin sensitive aminopeptidase (Psa).

Puromycin sensitive aminopeptidase

PSA is a ubiquitously expressed member of the M1 family of zinc metallopeptidases, proteolytic enzymes that catalyze the cleavage of the N-terminus of substrate proteins or peptides in the presence of a zinc cation cofactor (Taylor, 1993; Yao & Cohen, 1999). M1 aminopeptidases have identified roles in regulatory processes, including signaling, trafficking (through microtubule association), and antigen presentation (Lendeckel *et al.*, 2000; Stoltze *et al.*, 2000; Constam *et al.*, 1995). Orthologues of PSA have been found to be remarkably well conserved (Shulz *et al.*, 2001). A high degree of similarity (75%) between the catalytic domain of the fly, mouse, and human proteins suggest similar functions and substrates and highlights potential importance of the enzyme in cell processes (Figure 2) (Schultz *et al.*, 2001). In *C. elegans*, the protein is 36-37% identical to human PSA with key domains having higher levels of similarity (Lyczak *et al.*, 2006). *Psa* in mammals, and its orthologue dPsa in *Drosophila*, was first studied in

enkephalin degradation, but recent studies examining localization of PSA found it to be concentrated to the cytoplasm and nucleus, which argues against roles in digestion of extracellularly concentrated substrates (Menzies *et al.*, 2010; Hersh & McKelvy, 1981; Hui *et al.*, 1983). The localization of PSA, as well as its ability to digest diverse sequences, instead points to functions of proteasome product digestion, with some functionality in digestion of antigenic peptides for presentation on MHC Class I molecules (Menzies *et al.*, 2010; Constam *et al.*, 1995; Saric *et al.*, 2001; Stoltze *et al.*, 2004; Botbol & Scornik, 1983).

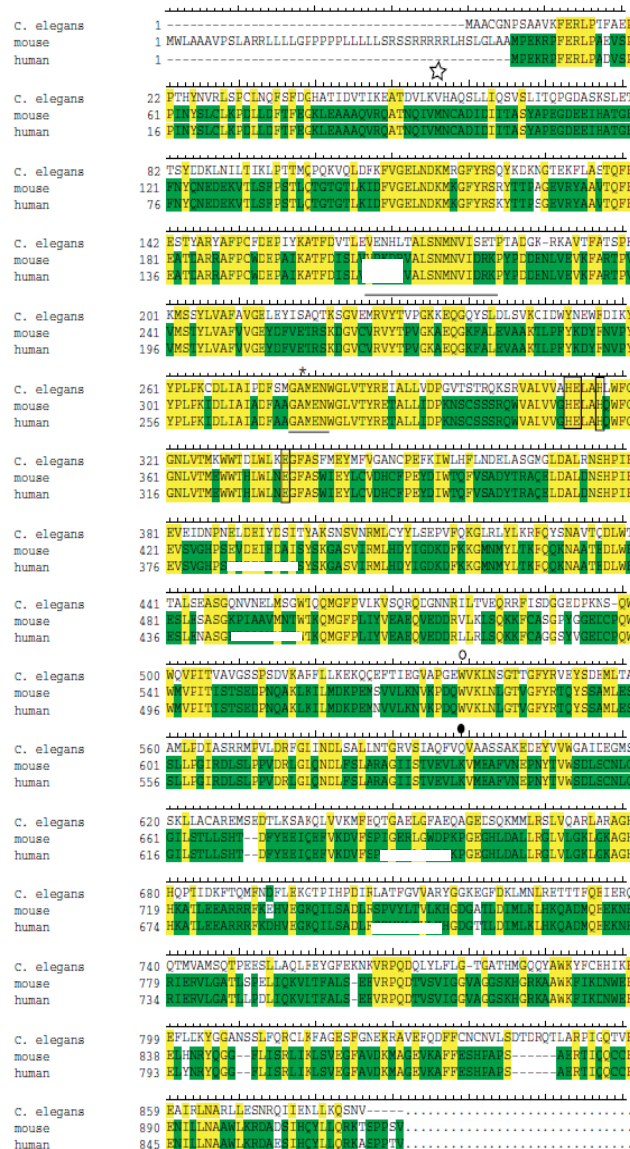


Figure 2: PAM-1 homology to Psa. (modified from Lyczak *et al.*, 2008) The amino acid sequence of PAM-1, mouse (GenBank AAH86798) and human (GenBank NP_0006301) orthologues of Psa. Colored blocks mark matches in amino acid sequence. Overlined area denotes homology with 26S proteasome subunits (Constam *et al.*, 1995).

Psa has also been implicated in the removal of cytotoxic protein aggregates in neurodegenerative diseases, such as polyglutamine peptides and huntingtin in cultured muscles with induced Huntington disease, aberrant SOD1 complexes in amyotrophic lateral sclerosis (ALS), and, most significantly, mutated tau proteins in Alzheimer disease mice models, although the effect of PSA on tau has been debated (Kita *et al.*, 2002; Karsten *et al.*, 2006; Ren *et al.*, 2011; Chow *et al.*, 2010; Kudo *et al.*, 2011). Overexpression of *Psa* was, in fact, neuroprotective against neurodegeneration caused by human *tau* aggregation in *Drosophila* models (Karsten *et al.*, 2006). It is suspected that although PSA protects against wild-type protein accumulation in the brain through proteasomal product degradation under normal conditions, the response it creates is a slow process and is not always effective (Menzies *et al.*, 2010). When the necessity for clearance becomes too high, or when the proteasomal products begin to build up and aggregate, PSA can act as an autophagic mediator for a more efficient clearance of aggregates (Menzies *et al.*, 2010). Interestingly, it has been shown that PSA also has the ability to induce autophagosome formation independently of its proteolysis activity (Krupa *et al.*, 2013). These studies have found PSA as a mediator of autophagy in both a proteolytic and proteolytic-independent manner.

Psa/PAM-1 in Fertility

Mutations in the *Psa* orthologues of different organisms result in meiotic errors in germ cells and are associated with reduced fertility (Osada *et al.*, 2001a; Osada *et al.*, 2001b; Schulz *et al.*, 2001; Hersh & McKelvy, 1981). Male *Drosophila* with *dPsa* deficiencies display reduced fertility, but an overexpression in the same organisms causes differentiating cell death (Schulz *et al.*, 2001). Surprisingly, *Drosophila dPsa* knockouts were viable (Schulz *et al.*, 2001). It is possible that, because of the neuroprotective roles of PSA, these organisms had neurological deficits that were undetectable – another potential selective pressure (Schulz *et al.*,

2001). Male mice that lack PSA are viable, but are infertile, lack copulatory behavior, and have a decrease in spermatogenesis (Osada *et al.*, 1999; Osada *et al.*, 2001a). Female mice with loss-of-function PSA alleles produce embryos with reduced viability (Osada *et al.*, 2001a; Osada *et al.*, 2001b; Towne *et al.*, 2008).

In the articles, the fertility defects in male mice were attributed to degeneration of Sertoli cells, and the subsequent neurological defects were caused by dysregulation of PSA-mediated involvement in maintenance of testosterone associated reproductive signal pathways (Osada *et al.*, 2001a). The fertility defects in female mice were attributed to defects in cell cycle function caused by lack of PSA (Towne *et al.*, 2008; Osada *et al.* 2001b). The fertility defects in *Drosophila* were attributed to dysregulation in decreased proteolysis metabolic targets (Schulz *et al.*, 2001). Though these are all possible causes of the observed defects, autophagic involvement in these phenotypes was not considered, and may provide an alternative mechanism of fertility regulation in these models. The potential roles of PSA in fertility could also help explain for the highly-conserved nature of the protein; the importance of the protein in fertility could be a selective pressure (Schulz *et al.*, 2001).

PAM-1, the *Caenorhabditis elegans* orthologue of mammalian PSA, also has known functions in fertility (Lyczak *et al.*, 2006). PAM-1 localizes to neurons and intestinal walls in larvae and adults, but has also been found to be expressed in embryos and in developing oocytes (Brooks *et al.*, 2003; Lyczak *et al.*, 2006; Cude & Trzepacz, unpublished). *pam-1* has been implicated in the mediation of oocyte meiosis exit and mitosis entrance through regulation of cyclin B3 inactivation (Lyczak *et al.*, 2006). PAM-1 has suggested roles in regulating microtubules and/or microtubule-associated proteins and, in this function, has been found to be a requirement of proper anterior posterior polarity (Lyczak *et al.*, 2006). Although a specific microtubule binding domain has not been characterized in *pam-1*, Psa has known microtubule binding domains and functions (Constam *et al.*, 1995). PAM-1

has therefore been described to have multiple targets for regulation of meiosis (Peer, 2011).

Mutations in *pam-1* cause a variety of phenotypes such as decreased embryonic viability, which could be explained by its roles in meiosis as well as other phenotypes that are not as easily explained by PAM-1's known roles of delayed nucleolar disassembly in developing oocytes and an expansion of the population of pachytene stage germinal nuclei (Althoff *et al.*, 2014). The apparent delay in development caused by *pam-1* mutations could be contributing to the decrease in brood size and embryonic viability that is also seen in worms harboring *pam-1* mutations. The subsequent question arises: what could be causing these developmentally delayed phenotypes in *pam-1* mutants?

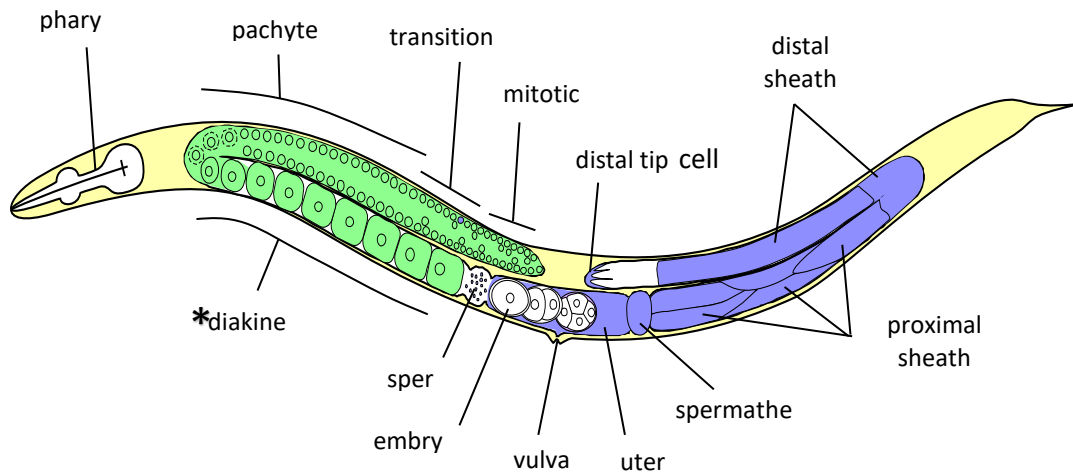


Figure 3: The *C. elegans* gonad. *C. elegans* have two identical gonads where oocytes mature and line up for exit. Nuclei divide mitotically at the distal end of the gonad. The nuclei then begin to transition to and enter pachytene. At approximately the bend in the gonad, where the proximal gonad begins, the nuclei enter diakinesis, where the cell membrane begins to form. The oocytes are then fertilized and exit the worm through the vulva. The asterisk denotes the gonadal location where culling occurs. The gonad on the left is showing the gonadal nuclei. The gonad on the right is showing the somatic sheath.

C. elegans have two identical U-shaped gonads where oocytes are produced and line up in an assembly line-like fashion before fertilization (*Figure 3*). Oocytes go through a variety of developmental stages before fertilization. The nuclei are first mitotically divided, after which they enter a transitional phase where chromosomes undergo homologous recombination and synaptonemal complex formation in preparation for meiosis (Hubbard & Greenstein, 2000). The nuclei then enter meiosis in the pachytene stage (Hubbard & Greenstein, 2000). The nuclei in this stage are not surrounded by a cell membrane, but instead exist in a shared cytoplasm termed a syncytium although a single nucleus and its surrounding cytoplasm is still often referred to as a germ cell (Hubbard & Greenstein, 2000). In wild-type animals, the germinal nuclei consistently exit pachytene at approximately the bend of the gonad through a condensation of chromosomes and enter a stage of diakinesis (Schedl *et al.*, 1997). During diakinesis, a cell membrane forms around the nuclei and the nucleolus disappears as preparation for fertilization (Schedl *et al.*, 1997). The oocyte is then fertilized by the sperm stored in the spermatheca and exits the gonad through the vulva (Schedl *et al.*, 1997).

It is estimated that about half of all germ cells produced are destroyed in the pachytene stage of development – only 300 oocytes are produced from 600 original nuclei (Schedl *et al.*, 1997). The nuclei to be degraded have been suggested to act as nurse cells to the surviving oocytes, providing nutrients and maternal factors (Gumienny *et al.*, 1999). Once the nurse cell function is fulfilled, the nuclei are no longer necessary and can be destroyed (Gumienny *et al.*, 1999). The selection of these functional nurse cells remains unclear, but the removal of excess nuclei has been suggested to occur through apoptosis (Hubbard & Greenstein, 2000). Apoptotic corpses are seen primarily in nuclei of the late pachytene stage, in the region of the gonad just distal to the loop region (Hubbard & Greenstein, 2000). Characterization of this cell death provides further support for an apoptotic mechanism. It is suggested that some fated nuclei condense the nucleus and

surrounding cytoplasm, aggregate the chromatin, and corpses are phagocytosed by the gonadal sheath cells after the event of a cell death (Hubbard & Greenstein, 2000). This process requires the apoptosis genes *ced-3* and *ced-4* (Gumienny *et al.*, 1999).

However, only approximately 50% of eliminated nuclei have been directly attributed to apoptosis (Hubbard & Greenstein, 2000). Prior studies have explained the discrepancies between visualized apoptotic nuclear degradation and total nuclear culling as problems with visibility of the corpses after apoptotic cell death (Hubbard & Greenstein, 2000). Contrasting this idea, however, is a study finding that defects in apoptosis do not affect the embryonic viability of *C. elegans* (Gumienny *et al.*, 1999). If apoptosis were to be defective, one would expect the functional nurse cells to develop into oocytes. The oocytes would compete for maternal factors, and embryonic viability would suffer. Interestingly, in *ced-3* and *ced-4* mutants, where no cell death can occur, there is no decrease in embryonic viability (Gumienny *et al.*, 1999). Similar results occur in mammalian systems; mice with mutations or knockouts causing defects in apoptotic machinery will develop and are fertile (Borsos *et al.*, 2011).

Autophagy in C. elegans fertility

One explanation for the inconsistency of apoptosis and viability is a second mechanism of nuclear destruction in the gonad called autophagy. Autophagy knockouts, including knockouts of *bec-1* (*C. elegans* orthologue of Atg6/Vps30) and *lgg-1* (*C. elegans* orthologue of Atg8), produce phenotypes more consistent with a defect in gonadal culling and subsequent deficiency in maternal factors. In worms homozygous for *lgg-1* or *bec-1* deletion mutations, a severe decrease in embryonic viability was evident, which is consistent with a potential role for autophagy in oogenesis (Sato & Sato, 2001; Schiavi *et al.*, 2013; Trinkwalder *et al.*, 2016). Interestingly, in worms with defects in both autophagy and apoptosis,

development was arrested and no viable embryos were produced (Borsos *et al.*, 2011). This data suggests a dual role of apoptosis and autophagy in oocyte nuclear destruction in the *C. elegans* gonad.

The selective degradation of the nucleus observed in germinal nuclei suggests the autophagy used in oogenesis is nucleophagy. The involvement of apoptosis in oocyte nuclear culling cannot be discounted, but it is likely autophagy and apoptosis collaborating to ensure optimum survival of the oocytes. Orthologues of Atg6 can regulate autophagic machinery in *C. elegans* and in mammals, and p53 is a known regulator for both processes (Liang *et al.*, 1998; Takacs-Vellai *et al.*, 2005; Tasdemir *et al.*, 2008). Consistently, under certain pathological conditions in the *C. elegans* embryo autophagy and apoptosis are co-regulated and redundantly required (Erdelyi *et al.*, 2010). Based on the phenotypes of autophagy and apoptosis mutants, nucleophagy may be the primary method for degradation. Degrading the autophagy has been characterized in fertilized embryos. There is not as much information known about autophagy in the gonad of *C. elegans* or any other organism.

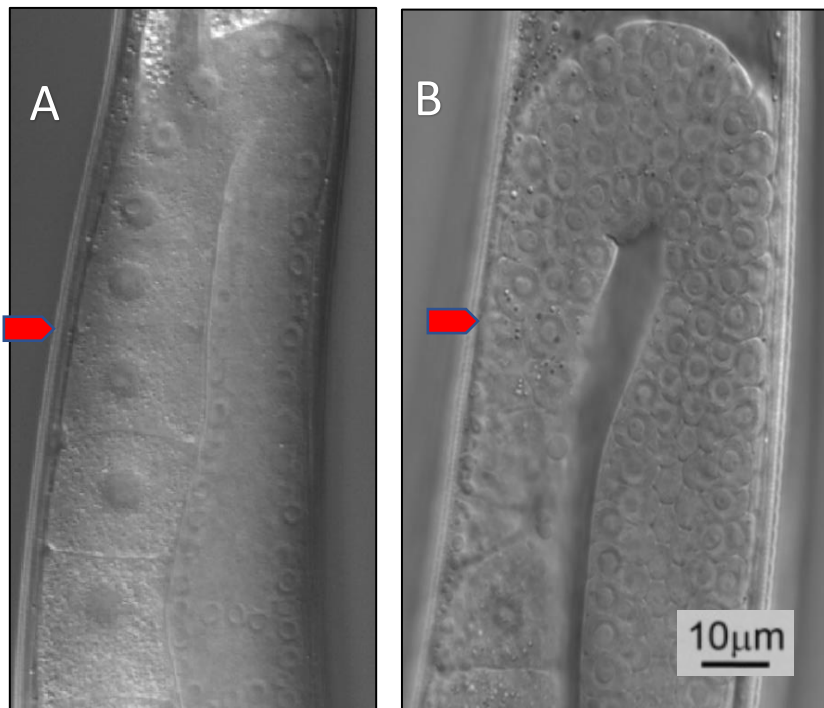


Figure 4: Pex phenotype. DIC images of two pam-1(ne4176) worms. The red arrows denote similar locations in the gonad. (A) The normal worm gonad. The arrow shows nuclei lined up and in diakinesis. (B) A gonad with the pachytene expanded (PEX) phenotype. The arrow shows nuclei competing for space, and in the pachytene stage.

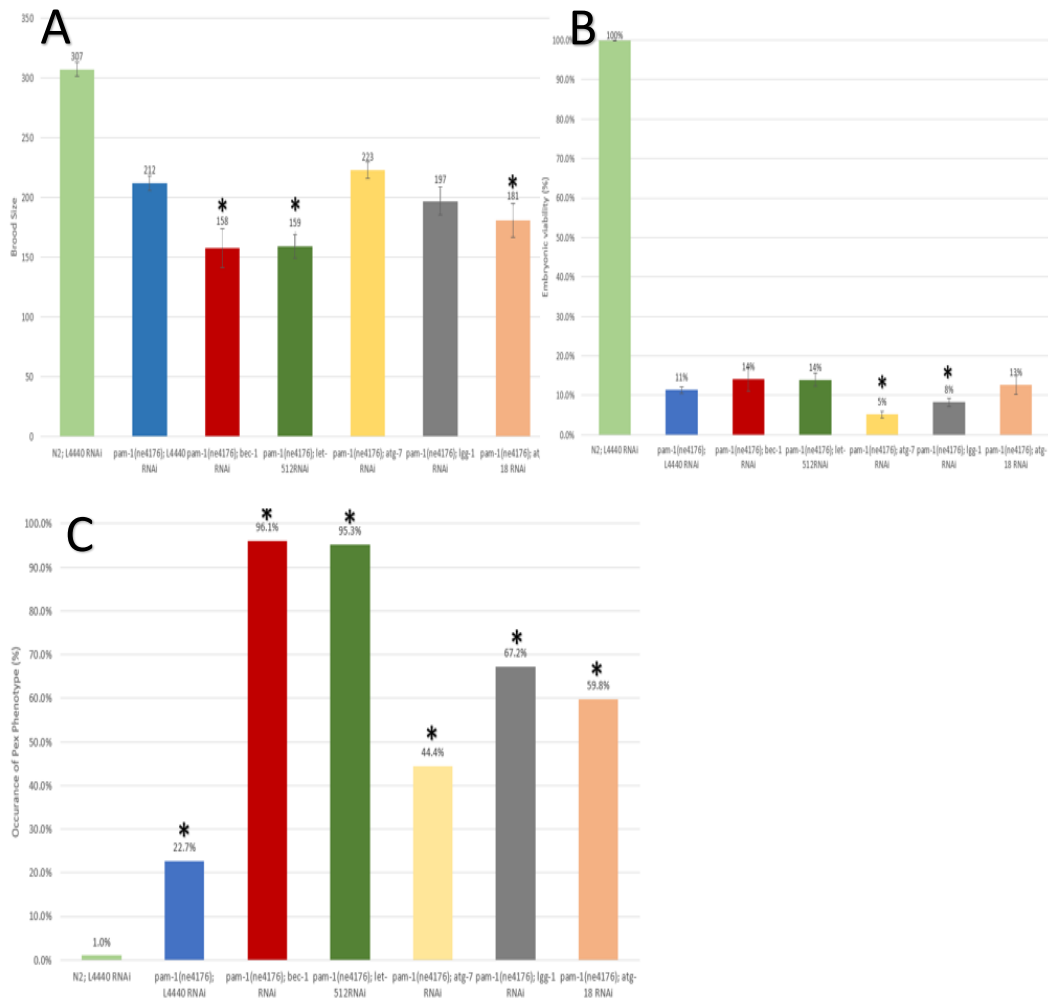


Figure 5: Occurrence of fertility defects in wild-type and pam-1 mutant worms under autophagic suppression. Autophagy was suppressed in wild-type (not shown) and pam-1 mutant worms via RNAi of independent autophagy genes. The empty vector L4440 was used as control. Brood sizes (A), embryonic viability (B), and the relative PEX occurrence in the gonad (C) was measured. Autophagy suppression in wild-type worms produced no phenotypes statistically different from wild-type (not shown). The pam-1 influenced fertility defects were exacerbated during autophagic suppression in worms harboring a pam-1 mutation, with a severe exacerbation of the PEX phenotype (C). The synergistic nature of the exacerbation suggests PAM-1 is collaborating with the autophagic process in *C. elegans* oogenesis. Statistics were calculated using a two-tailed T-test.

Previously collected data has found a possible relationship between PAM-1 and autophagy in the oogenesis of *C. elegans*. A synergetic reduction in brood size and embryonic vitality and, most notably, an expansion of the population of pachytene stage nuclei (PEX phenotype, *Figure 4*) was seen when the expression

of *lgg-1*, *bec-1*, *let-512* (orthologue of Vsp-34 in the PtdIns-3-kinase complex), *atg-17* (an E1 ubiquitin-activating-like enzyme involved in phagophore elongation) and *atg-18* (associates with the PAS in elongation) were independently suppressed (*Figure 1*) using RNAi in a mutant *pam-1(ne4176)* background (*Figure 5*). The same assay in a wild-type background produced no significant changes from wild-type, as the embryonic viability was measured at around 300 progeny and the embryonic viability was consistently measured at 99% (data not shown). The PEX phenotype was observed in insignificant amounts (data not shown).

The synergetic and significant reduction of brood size and embryonic viability and an increase in the PEX phenotype in the *pam-1* mutant background supports a model where PAM-1 and autophagy collaborate in germ cell nucleophagy (Cude & Trzepacz, unpublished). The mechanisms of this collaboration are unknown. Inquiry into the role of PAM-1 and autophagy in oogenesis, as well as the mechanisms of their collaboration, is needed to clearly characterize *C. elegans* oogenesis and oocyte nuclear degradation. Based on previous findings, PAM-1 is suspected to localize to autophagosomal structures around the nuclear membrane. The localizations will be apparent only in the cells that are acting as nurse cells and will undergo autophagy, creating differential expression around certain nuclei. PAM-1 would also be expected to be more highly expressed in models where autophagy is upregulated. The findings of these further investigations may provide more insight into regulation of autophagy via *Psa/pam-1* and, potentially, insight into regulation of oogenesis in higher eukaryotes.

Methods

Maintenance of C. elegans strains

Caenorhabditis elegans strains utilized included a wild-type N2 strain, *pam-1(ne4176)*, a missense allele on chromosome IV in the catalytic domain of the *pam-*

I gene isolated from a genetic screen for conditional embryonic lethal alleles (Pang *et al.*, 2004), and *pam-1(or282)*, a putative null 591bp deletion of the catalytic domain described previously (Lyczak *et al.*, 2006). All *C. elegans* strains were fed with *E. coli* strain OP50 and maintained at 20°C on 35mm plates of Nematode Growth Media (NGM), which consist of 50mM NaCl, 0.25% peptone, 1mM CaCl₂, 25mM KH₂PO₄, 1mM MgSO₄, 5µg/mL cholesterol, and 1.7%(w/v) agar, as described by Brenner (1974).

Construction of GFP transgene TRZ17

To construct the *pam-1p::GFP::pam-1* transgene, the GFP sequence was cloned into the a 10kb *pam-1* translational fusion construct plasmid that had the *C. elegans* genomic sequence of *pam-1* (figure 6). The sequence of *pam-1* used included the entire 3' UTR and the promoter, and the GFP sequence was cloned into the C-terminal region of the protein, directly after the ATG codon. Due to the large size of the plasmid and a lack of usable restriction sites, the necessary sequences were transferred to a MosSci single site integration vector to then amplify and anneal together using NEBuilder HiFi DNA assembly kit. After synthesis, the gene was sequenced and verified. The plasmid was then sent to a commercial transgenic facility (Knudra) for a single site integration into Chromosome I. The resulting transgenic strain, with the endogenous *pam-1* sequence on chromosome IV and a fluorescent protein tag on a *pam-1* sequence on chromosome I, was named TRZ17.

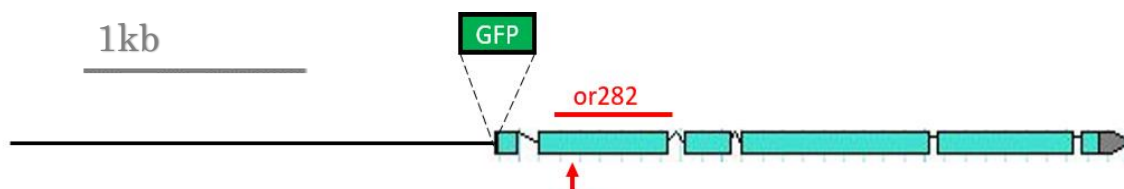


Figure 6: Genomic map of *pam-1*. The genomic map for *pam-1*, including the 3' UTR and the promoter. GFP sequence was cloned into the 3' end of the first intron, placing GFP at the C-terminal end of the protein. The two alleles used are shown in red.

Cross of TRZ17 into *pam-1* mutant strains

To cross the functional *pam-1* gene out of the TRZ17 strain, L4 hermaphrodites from DR439, homozygous for *dpy-20* (e49) and *unc-8* (e1282) mutations that bracket functional *pam-1* on chromosome IV, and males of the transgenic strain TRZ17, homozygous for functional *pam-1* on

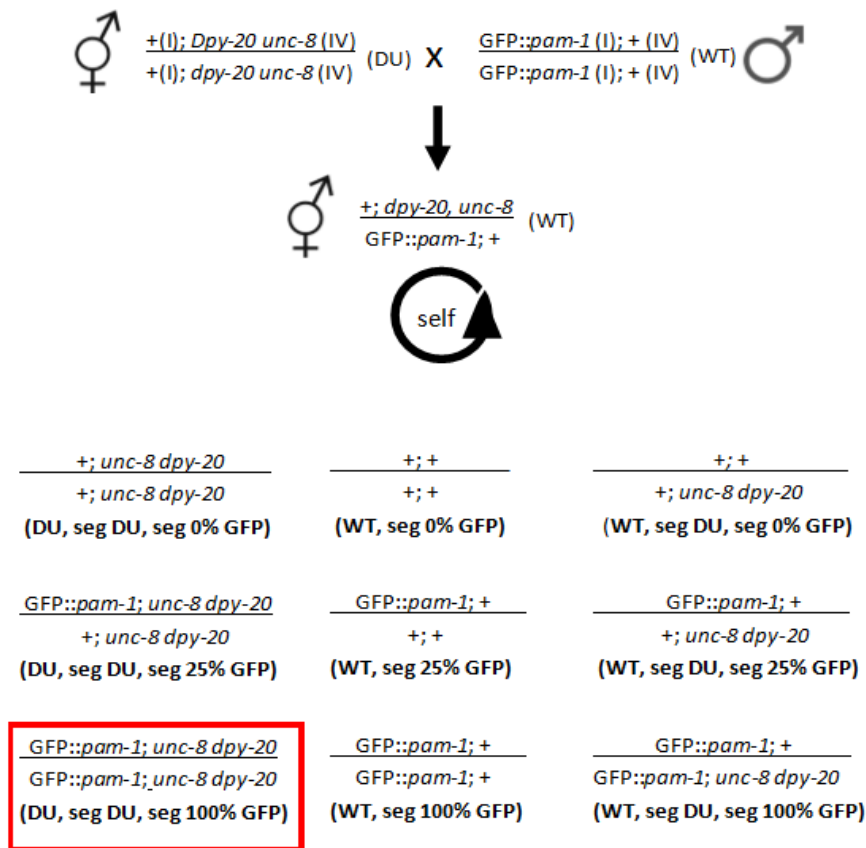


Figure 7: The genetic cross between *dpy-20 unc-8* worms and the transgenic *GFP::pam-1*. A diagram of the original cross between *dpy-20 unc-8* worms and the transgenic *GFP::pam-1* is shown above. The worms were crossed and the F1 generation was allowed to self-fertilize. The resulting genotypes are shown at the bottom. The phenotypes are shown bolded beneath the respective genotype. The red box indicates the desired population.

chromosome IV and *pam-1-p::GFP::pam-1* on chromosome I, were isolated on a 35mm NGM plate with a small (<3mm) area of concentrated food (referred to as a feeding plate) to concentrate worms to promote male fertilization of

hermaphrodites (Figure 6). Cross progeny hermaphrodites from the F1 generation had wild-type movement and were segregated before maturity to self-fertilize. In the F2 generation, progeny that displays dumpy, uncoordinated phenotype that defines homozygosity the *dpy-20* and *unc-8* mutations were segregated before

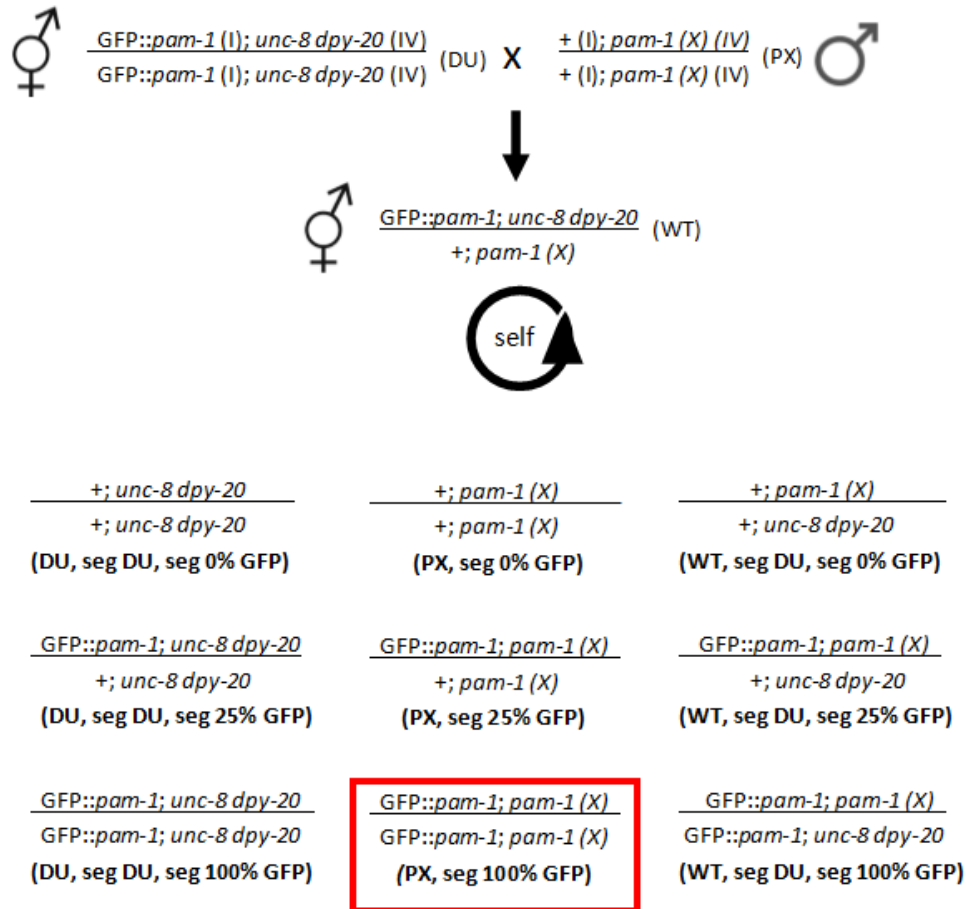


Figure 8: The genetic cross between *GFP::pam-1; dpy-20 unc-8* worms and *pam-1* mutants. A diagram of the cross between *GFP::pam-1; dpy-20 unc-8* worms and *pam-1(or282)* and *pam-1(ne4176)*, denoted as *pam-1(X)* is shown above. The worms were crossed and the F1 generation was allowed to self-fertilize. The resulting genotypes are shown at the bottom. The phenotypes are shown bolded beneath the respective genotype. The red box indicates the desired population.

maturity and allowed to self-fertilize. The F2 worms that showed GFP expression in 100% of the F3 progeny were deemed to be of the *unc-8 dpy-20; pam-lp::GFP::pam-1* genotype (Figure 7). Hermaphrodites of *unc-8, dpy-20; pam-lp::GFP::pam-1* were then isolated on a feeding plate and crossed with *pam-1(or282)* or *pam-1(ne4176)* males (Figure 8). Cross progeny hermaphrodites of the F1 generation had wild-type movement and were segregated before maturity and allowed to self-fertilize. In the F2 generation, about 75% of the progeny had wild-type movement. These worms were independently segregated before maturity and allowed to self-fertilize. The F2 worms that produced a population with no dumpy and uncoordinated phenotypes were considered to be homozygous for the

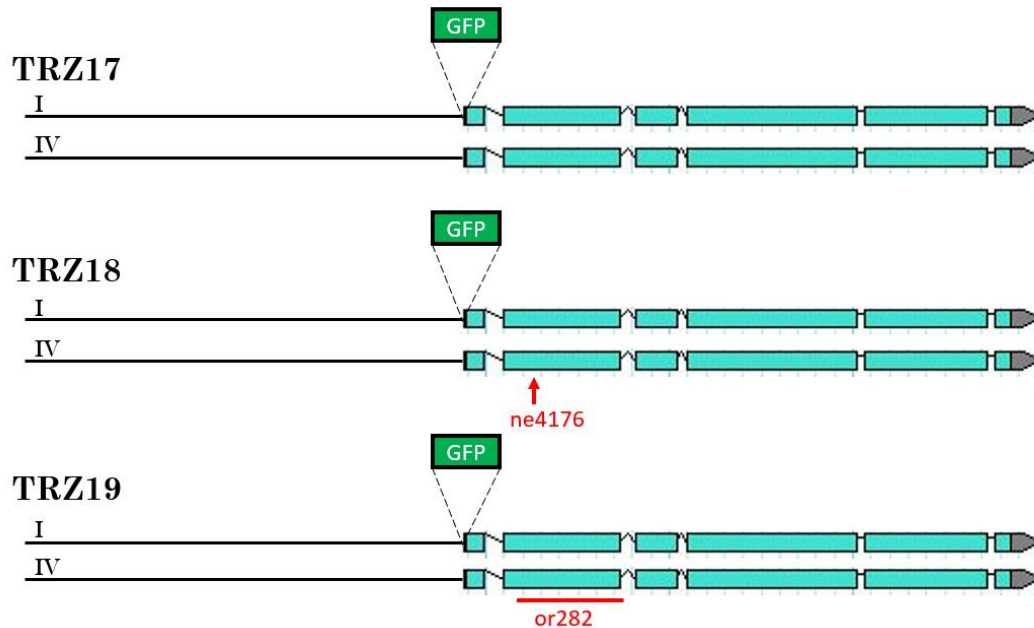


Figure 9: Genomic map of the three transgenes produced. The genomic map of the three transgenes created are shown above. Both chromosomes are shown. GFP insertion into chromosome I is denoted. Different alleles of the endogenous *pam-1* sequence on chromosome IV are shown in red.

respective *pam-1* mutation. The populations of progeny from these *pam-1* homozygous F2 isolates that displayed 100% GFP expression were deemed to be of the *pam-1(ne4176); pam-lp::GFP::pam-1* or *pam-1(or282); pam-lp::GFP::pam-1* genotype (Figure 8). The *pam-1(ne4176); pam-lp::GFP::pam-1*

strain was designated TRZ18 and the *pam-1(or282); pam-1p::GFP::pam -1* strain was designated TRZ19.

Fecundity of PAM-1 transgenic strains

The fecundity of the transgenic PAM-1 was determined by assessing the relative brood sizes, embryonic viability, and PEX occurrence of adult worms. The brood sizes and embryonic viability of the worms were assessed by segregating L4 hermaphrodites and assessing the number of embryos produced over the course of 3-4 days, or until no additional offspring were produced. Total brood size was described as the number of embryos laid by a single hermaphrodite. The embryonic viability was determined by dividing the number of embryos hatched by the total brood size. The occurrence of the PEX phenotype in a strain was determined by dividing the number of gonads with the PEX phenotype by the total gonads examined. The gonadal nuclei were observed using DAPI staining (below) and the PEX phenotype was determined to be present if nuclei past the bend in the gonad were in the pachytene stage of development.

RNA interference procedure

Independent inhibition of autophagy genes *lgg-1* and *bec-1* was accomplished using RNA-mediated interference (RNAi) (Fraser *et al.*, 2000; Kamath *et al.*, 2003). RNAi was performed using amplified nucleotide segments from *lgg-1* and *bec-1* exonic sequences. The sequences were inserted into the *C. elegans* RNAi feeding vector L4440 (Timmons & Fire, 1998) and transformed into *E. coli* strain HT115, an RNaseIII-deficient strain that carries an integrated T7 polymerase under inducible control of the *lac* promoter (Timmons *et al.* 2001).

HT115 competent cells were made by inoculating 250mL of LB medium with 1mL of HT115 stock and growing overnight at 20°C to an OD_{600nm} of 0.3. The resulting medium was spun at 3000rpm at 4°C for 10 minutes. The supernatant

was discarded and the bacterial cells were resuspended in 80mL of ice cold CCMB80 buffer, consisting of 10mM KOAc, 80mM $\text{CaCl}_2 \cdot 2\text{H}_2\text{O}$, 20mM $\text{MnCl}_2 \cdot 4\text{H}_2\text{O}$, 10mM, $\text{MgCl}_2 \cdot 6\text{H}_2\text{O}$, and 10% glycerol. This solution was incubated on ice for 20 minutes before centrifuging down as before. The cells were again resuspended in 10mL of ice cold CCMB80 buffer and frozen at -80°C until use. The bacterial strain that resulted from transformation into these cells expressed an inducible RNA duplex (RNAi food) for each gene. The RNAi food was plated on NGM supplemented with $50\mu\text{g/mL}$ kanamycin and 1mM IPTG.

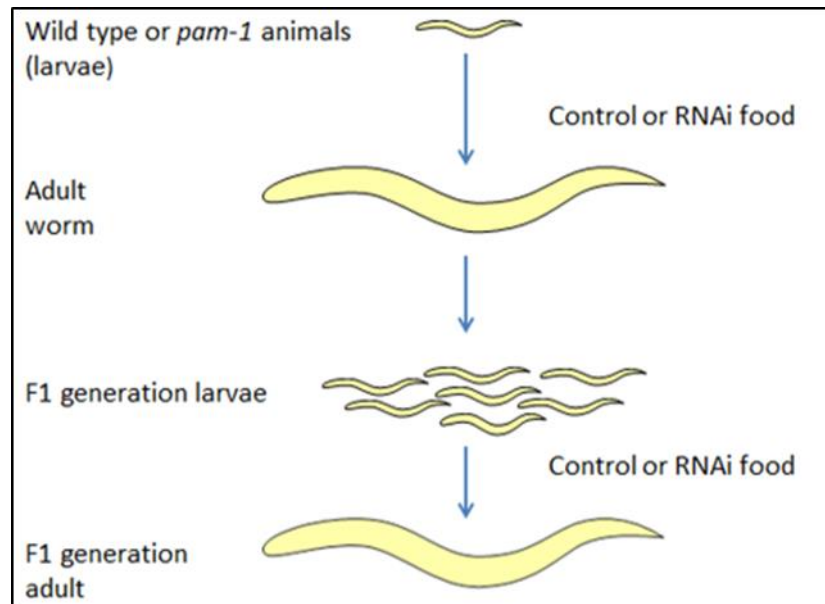


Figure 10: Experimental design of autophagy suppression via RNAi. Two generations of worms were grown on RNAi food seeded 35mm plates.

Synchronized L1 animals were obtained by dissolving adult hermaphrodites in a 7:2:1 solution of water:bleach:5M KOH to release the embryos, followed by several washes with M9 and incubation in M9 with gentle rocking overnight. The L1 worms were plated on the RNAi seeded plates and grown to adulthood. Worms of the F1 generation were moved to fresh RNAi seeded plates and grown to

adulthood (*Figure 10*). Random adults of the F1 generation were selected for expression assays.

Starvation procedure

Autophagy was induced by starvation of adult worms. Briefly, hypochlorite synchronized control and *bec-1* RNAi treated TRZ19 L1s were plated on NGM and grown to young adulthood (~60 hrs.). Adult hermaphrodites were washed with M9 and plated on starvation plates, which were NGM plates with excluded peptone to reduce growth of bacteria. After 24 hours, worms were randomly selected for expression assays.

In vivo fluorescent microscopy

In vivo imaging of fluorescent transgenes and stains was done on a Olympus BX51 microscope outfitted with Nomarski optics. Worms were picked onto a 2% agarose gel pad and exposed to 0.1mM of sodium azide for paralysis. Images were acquired with a Hamamatsu (CCD camera) equipped with the appropriate filters to detect GFP, RFP, and DAPI signals.

Nile Red staining

Nile red dye was used to stain tissue fats to assess the efficiency of the starvation protocol (Pino *et al.*, 2013). Starved TRZ19 worms and well-fed TRZ19 worms were removed from the plates using 1xPBS with 1% triton. The worms were then washed with water. After settling on ice, a second water wash was performed. The worms were then exposed to 40% isopropanol for three minutes to fix and then the supernatant was removed from the settled worms.

A Nile Red/isopropanol solution was made from 6μL of the Nile Red stock (0.5mg/mL in acetone) per 1mL of 40% isopropanol. Worms were incubated in the Nile Red/isopropanol solution for 30 minutes at 20°C with gentle rocking in the

dark. Worms were spun down and washed with M9 solution. Stain was viewed using *in vivo* fluorescent microscopy as described previously. DAPI staining was used to visualize germ cell DNA. Worms were incubated in ethanol for 30-60 seconds for fixing, followed by rehydration in M9. DAPI (Sigma) was added to the M9 in a 1/1000 dilution. Stain was viewed using *in vivo* fluorescent microscopy as described.

Results

Fecundity of PAM-1 transgenic strains

Fecundity assays of TRZ17, TRZ18, and TRZ19 suggest that the transgenes functionally rescue PAM-1 induced phenotypic deficiencies to wild-type or better numbers (Table 1). In TRZ17, brood size was found to be similar to wild-type (Figure 11A, $p=0.657$). Given that TRZ17 has the functional endogenous copy of *pam-1*, functionality of the transgene would not be necessary for rescue in this strain. TRZ18 and TRZ19 each had a mutant *pam-1*, with levels of functionality

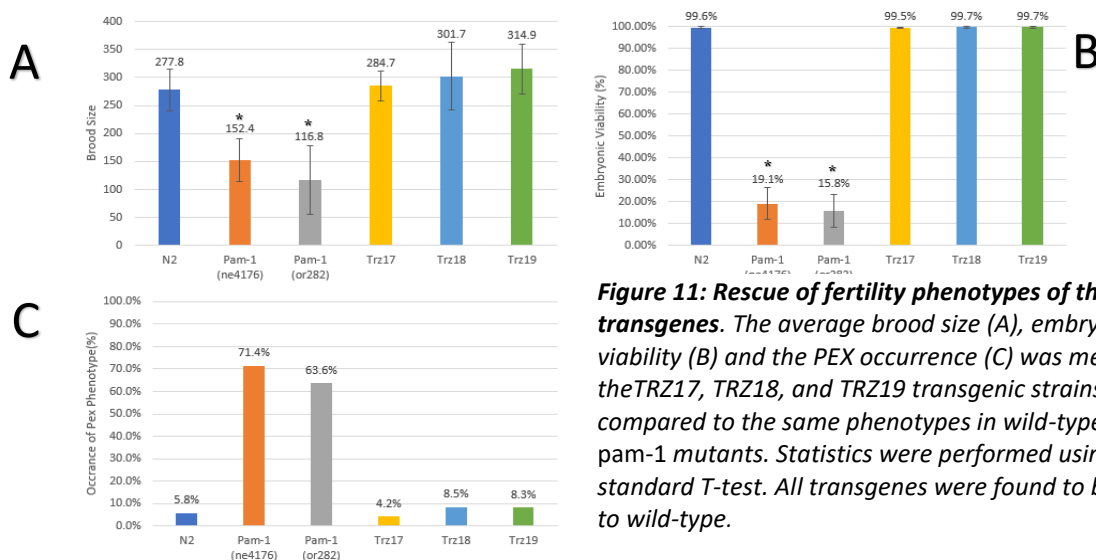


Figure 11: Rescue of fertility phenotypes of the transgenes. The average brood size (A), embryonic viability (B) and the PEX occurrence (C) was measured in the TRZ17, TRZ18, and TRZ19 transgenic strains, and compared to the same phenotypes in wild-type and *pam-1* mutants. Statistics were performed using a standard T-test. All transgenes were found to be similar to wild-type.

markedly lower than wild-type, and the transgene. These strains made for a better

model of testing the rescue of the transgene. The brood size of these two strains were also similar to wild-type (*Table 1*, $p=0.319$ and $p=0.075$, respectively). These trends continued in all strains when looking at embryonic viability and the persistence of the PEX phenotype. The transgenic strains were statistically similar to wild-type ($p>0.05$), and statistically different than *pam-1(ne4176)* and *pam-1(or282)* ($p<0.05$, *Figure 11B-C*, *Table 1*).

Strain	Sample size (BS and EV/PEX)	Brood Size	P values from N2	Embryonic Viability	P values from N2	PEX occurrence	P values from N2
N2	2499/52	277.8		99.6%		5.8%	
<i>pam-1</i> (<i>ne4176</i>)	2286/42	152.4	<0.01	19.1%	<0.01	71.4%	<0.01
<i>pam-1</i> (<i>or282</i>)	1168/66	116.8	<0.01	15.8%	<0.01	63.6%	<0.01
Trz17	2562/48	284.7	0.657812	99.5%	0.696272	4.2%	0.72
Trz18	3017/59	301.7	0.318735	99.7%	0.544684	8.5%	0.58
Trz19	2834/48	314.9	0.075033	99.7%	0.729565	8.3%	0.625

Table 1: Fecundity metrics of worms used in this study. Table showing the brood sizes, embryonic viability, and PEX occurrence in the different strains. Statistics were performed using a standard T-test. Sample sizes are shown in the left column.

PAM-1 localizations in normal environment

Normal state gonadal localizations of PAM-1 in TRZ17, TRZ18, and TRZ19 were identical. PAM-1 was found to be expressed in the gonadal nuclei (*Figure 12*). The visualization of PAM-1 in the gonad was difficult, as the expression was faint

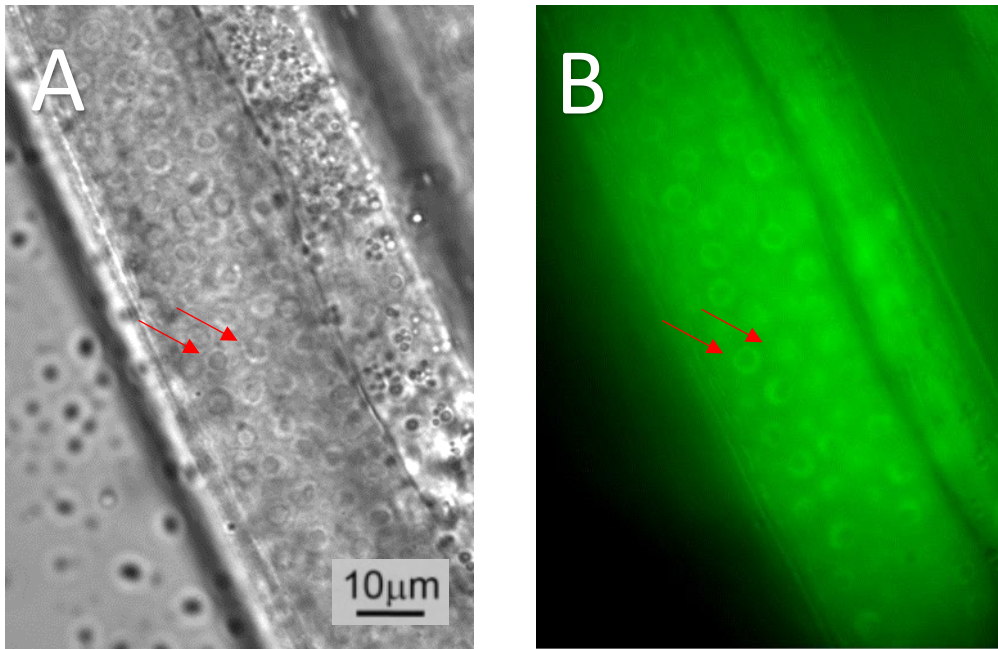


Figure 12: Steady state localizations of GFP::pam-1 in TRZ19. Localizations of GFP::pam-1 are shown above. (A) DIC image of TRZ19 gonad. (B) GFP::pam-1 localizations in the same gonad. Arrows show differential expression in nuclei.

and was quickly bleached (<5 sec). There did not appear to be any differential expression in the different regions of the gonad, except that PAM-1 expression became more diffuse after formation of the cell membrane in diakinesis (not shown). This is indicative of PAM-1 diffusion into the cytoplasm after oocyte membrane formation. The regions of the gonad in which PAM-1 was most highly expressed was around the bend in the gonad, which coincided with late

pachytene/transition to diplotene. In over 60 gonads visualized, this phenotype was evident 100% of the time.

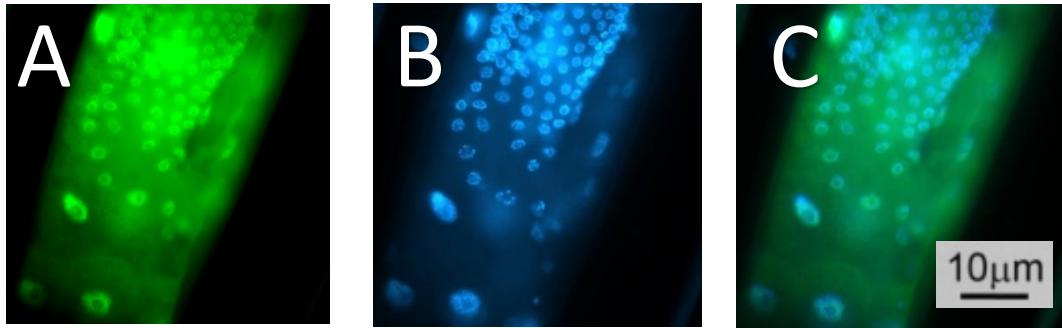


Figure 13: Nuclear localizations of GFP::pam-1. GFP::pam-1 was confirmed to be localized to gonadal nuclei. (A) GFP::pam-1 expressions. (B) DAPI stain. (C) An overlay of the GFP and DAPI stain.

There appeared to be differential expression of PAM-1 in specific nuclei – some displayed a more intense signal than the others (*Figure 12B*). There was not an obvious pattern as to which nuclei had a stronger expression. In some of the nuclei with stronger GFP::PAM-1 expression, there appeared to be a slight perinuclear accumulation; the signal was concentrated in the periphery of the nucleus. Approximately 50% of the nuclei displayed a more pronounced nuclear signal, while a smaller subset (10%) displayed a perinuclear staining pattern (n=70). These localizations were confirmed using DAPI staining (*Figure 11*).

PAM-1 localizations in autophagy suppressed environment

Because of the similarities of TRZ17, TRZ18, and TRZ19 in expression and functionality, only TRZ19 was used in all subsequent studies. TRZ19 is homozygous for the transgenic copy of functional *pam-1* and was homozygous for the non-functional *pam-1(or282)* deletion mutation.

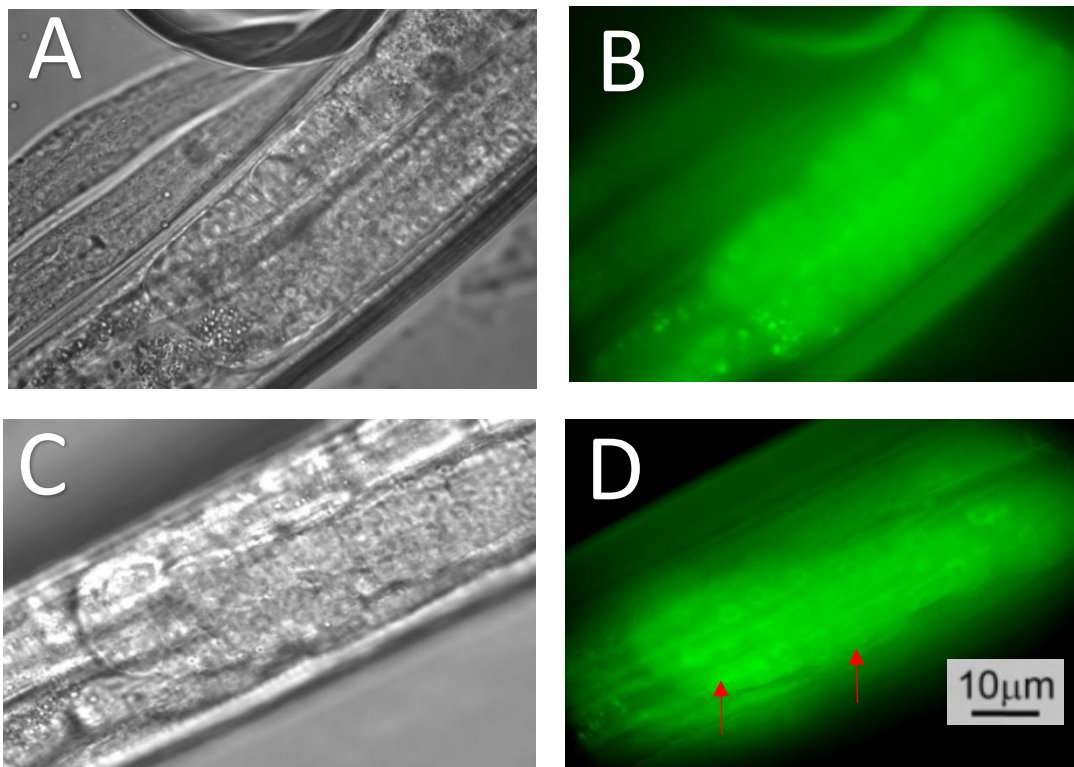


Figure 14: GFP::pam-1 localizations in an autophagy suppressed environment in TRZ19. Autophagy was suppressed via independent *lgg-1* and *bec-1* RNAi. (A-B) Worms subject to *lgg-1* RNAi (A) DIC image of TRZ19. (B) GFP::pam-1 localizations in the same worm. (C-D) Worms subject to *bec-1* RNAi. (C) DIC image of TRZ19. (D) GFP::pam-1 localizations in the same worm. Arrows show perinuclear accumulation of GFP::pam-1.

Suppression of *bec-1* and *lgg-1* by RNAi did not have an effect on the localization of GFP::PAM-1 (Figure 14). GFP::PAM-1 remained localized to the nucleus, and there was some slight perinuclear accumulation. The signal was the strongest in the pachytene stage nuclei, and dissipated in diakinesis.

A differential expression between nuclei was not evident. However, there did appear to be an upregulation of PAM-1 in these worms. When visualizing the localizations, the GFP signal was not as faint and did not bleach as quickly as in the normal state. The signal last for about 30 seconds, making the localizations easier to study.

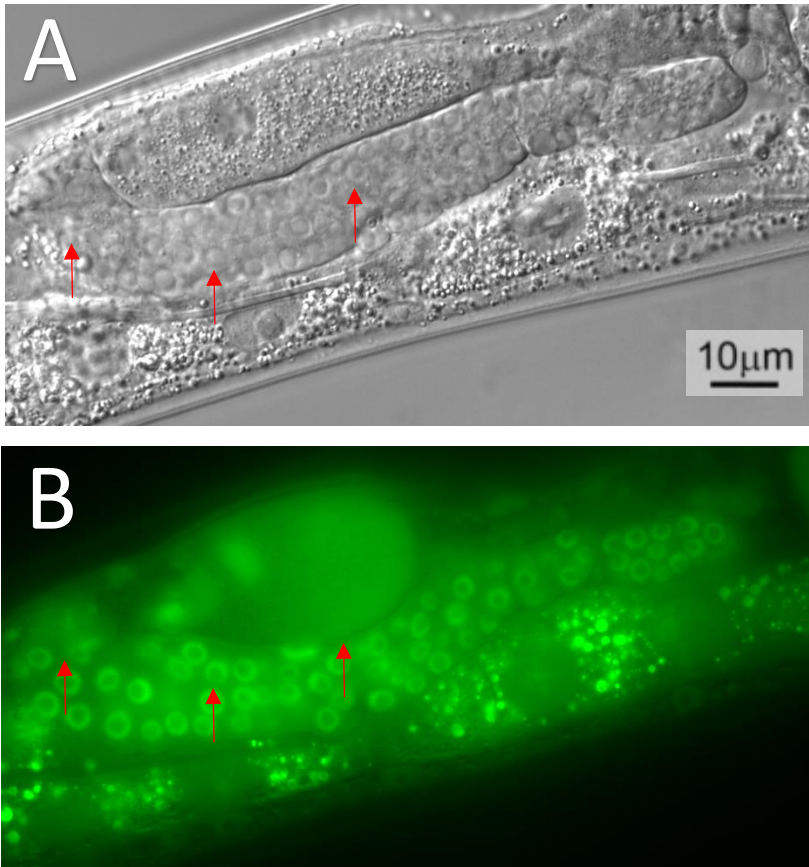


Figure 15: GFP::pam-1 localizations in an autophagy stimulated environment in TRZ19. Autophagy was stimulated by starvation. (A) DIC image of starved TRZ19. (B) GFP::pam-1 localizations in the same worm. Arrows show examples of perinuclear accumulation of GFP::pam-1 and the same nuclei in DIC.

PAM-1 localizations in autophagy stimulated environment

Induction of starvation was confirmed by loss of stain by the lipophilic dye Nile Red. Starvation appeared to increase the fluorescent intensity of the GFP::PAM-1 signal in all gonadal nuclei (*Figure 15*). The intense signal made visualization simple. The increased signal was not associated with a change in gonadal localization, as PAM-1 was still concentrated in the pachytene stage nuclei. However, starvation resulted in an increase in the perinuclear localization of GFP::PAM-1. More gonadal nuclei showed a perinuclear concentration within the nucleus than wild-type (*Figure 15B*). The nuclei that had the perinuclear accumulation were concentrated to the pachytene stage, which extended past the bend in the gonad in the starved worms. In diakinesis stage nuclei, PAM-1 appeared

to dissipate within the nucleus, presenting a strong nuclear localization, and then dissipate within the cytoplasm of the forming oocyte (not shown). This gonadal localization was observed in all autophagic models examined, but most evident in the autophagy stimulated environment.

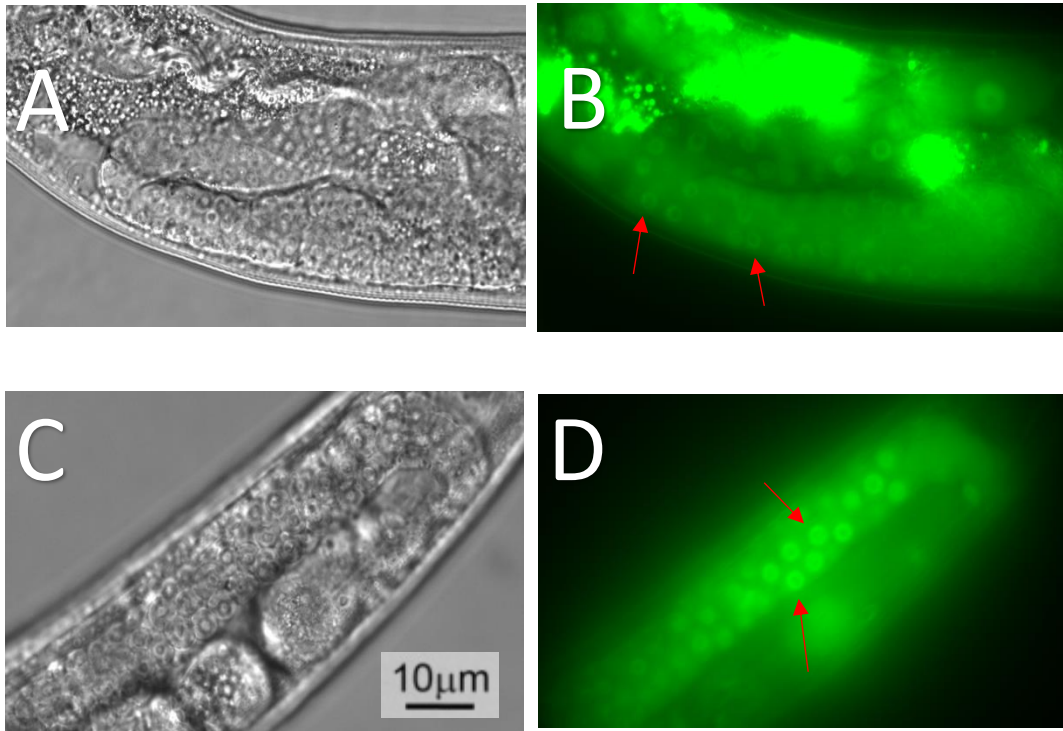


Figure 16: Increased GFP::pam-1 expression in starved worms is independent of autophagy. Autophagy was suppressed via independent *lgg-1* and *bec-1* RNAi. The worms were then subject to starvation to stimulate an autophagic response. (A-B) Worms subject to *lgg-1* RNAi and then starved (A) DIC image of TRZ19. (B) GFP::pam-1 localizations in the same worm. (C-D) Worms subject to *bec-1* RNAi and then starved. (C) DIC image of TRZ19. (D) GFP::pam-1 localizations in the same worm. Arrows show perinuclear accumulations of GFP::pam-1.

PAM-1 localizations in autophagy suppressed worms in a stimulated environment

Some worms were exposed to *bec-1* RNAi food and then subsequently starved after reaching adulthood. Because of the similar expressions in *bec-1* and *lgg-1* RNAi, worms exposed to *lgg-1* RNAi were not starved. PAM-1 in this environment did appear to have a similar upregulation to starvation only models (Figure 16).

Localizations of PAM-1 were also very similar to starvation models, but perinuclear localization occurred at a lesser extent (*Figure 16*). No other differences were observed.

Discussion

The first goal of the project was to test the rescue of the transgenic strains. TRZ17, TRZ18, and TRZ19 were found to be functionally identical to wild-type. TRZ17 was homozygous for a functional, non-transgenic *pam-1*. However, TRZ18 and TRZ19 did not have a functional endogenous copy. The TRZ18 and TRZ19 strains were crossed into *pam-1(ne4176)* and *pam-1(or282)* mutant backgrounds, respectively, eliminating the functionality of the endogenous gene. These mutations in wild-type worms caused severe deficiencies in the brood size, embryonic viability, and PEX phenotype. However, when crossed with the transgenic strain, the transgene was found to rescue fecundity phenotypes to wild-type levels. TRZ18 and TRZ19 were found to be statistically similar to TRZ17 and wild-type, even though the strains were homozygous for *pam-1(ne4176)* and *pam-1(or282)* mutations respectively. The similarities of TRZ17, an overexpression model, to

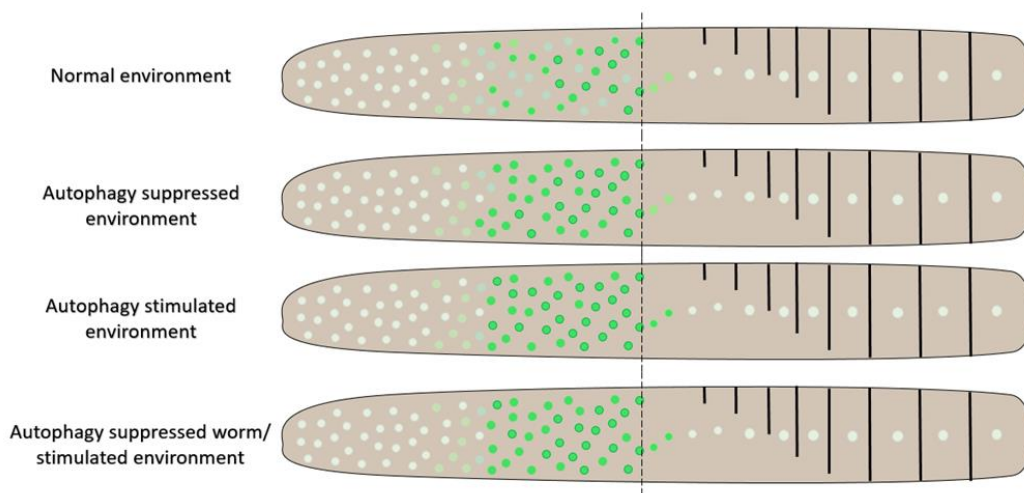


Figure 17: GFP::pam-1 localizations in autophagy models. The figure above depicts the phenotypes observed in the different autophagy models.

TRZ18 and TRZ19 suggested that overexpression of PAM-1 does not influence phenotypes.

The localizations of PAM-1 were then studied to further differentiate the protein's role in both autophagy and fertility. The localizations of PAM-1 to the nucleus during pachytene, where nuclei are undergoing prophase of meiosis I, did not support the hypothesis of *pam-1* localizing to the outside membrane of the nucleus, but did support previous studies finding PSA localizes to the nucleus during mitotic prophase (Constam *et al.*, 1995). The perinuclear localization of PAM-1 and the increase of this localization in starvation models were surprising observations. The perinuclear accumulation of PAM-1 gave some insight into the protein's role in autophagy.

Autophagosomes are known to be delivered to the outer nuclear membrane by a microtubule network (Korolchuk & Rubinszein, 2011). During starvation, more autophagosomes accumulate in the perinuclear area because they are recruited by lysosomes, which rapidly accumulate perinuclearly in these conditions (Jahreiss *et al.*, 2008; Korolchuk *et al.*, 2001). PAM-1 localizations match the autophagosome localizations in these conditions. PAM-1 has a slight perinuclear expression in normal state, but this expression is markedly increased in starvation conditions. These data suggest potential colocalizations of autophagosomes and PAM-1 in models where autophagy is upregulated. However, the perinuclear localization in autophagy suppressed worms contradicted this model. Further studies in a cell culture system which use larger cells with clearer cellular anatomy, or with a *lgg-1* marker, could confirm or reject a colocalization and could further explain the phenotype in RNAi-treated worms. It is important to note that many of the worms of the starvation phenotype bagged, or did not lay their embryos. Their embryos hatched inside the parent and survived on the nutrients within the mother

until the cuticle was digested and the progeny could exit. At 24 hours, this phenotype affected the gonad slightly, and could have affected our results.

Worms that harbor *pam-1* mutations are known to have low embryonic viability, smaller brood sizes, and delays in development seen by the position of oocyte nucleolar disassembly and the expansion of pachytene stage germinal nuclei (Cude & Trzepacz, unpublished). In worms with a GFP::*pam-1* transgene, the gonadal localizations of PAM-1 showed it to be expressed to the greatest degree around the bend inside the gonad in pachytene stage nuclei. This gonadal location is where the nuclear culling occurs. After pachytene, when the cells are lined up in the gonad and undergo diakinesis, PAM-1 becomes more diffuse and no longer has a nuclear or perinuclear localization. In addition, there appears to be differential expression of PAM-1 between nuclei in the normal state. About 50% of the nuclei appeared to have higher levels of PAM-1, however, a more quantitative form of measurement should be used to confirm these differential expressions. Given the brief nature of the transgenic signals, an antibody to GFP should be employed to confirm the accuracy and validity of the observation.

Taken together, these data further support a model where PAM-1 participates in the culling of gonadal nuclei functioning as nurse cells by autophagy to promote maturation of remaining oocytes (*Figure 18*). In this model, *pam-1* mutations would hinder activation of autophagy in pachytene stage nuclei, and thus functional nurse cells would not be degraded, leaving the remaining nuclei with more competition for nutrients and maternal factors. PAM-1 would be expected to be expressed to the highest degree in nuclei of the pachytene stage about to undergo nucleophagy, which would explain the differential nuclear expression. PAM-1 would also be expected to be upregulated when autophagy is upregulated, or when autophagy is needed. Further supporting this model, the more intense GFP::PAM-1 signal suggests an upregulation of PAM-1 in the starved worms. In starvation

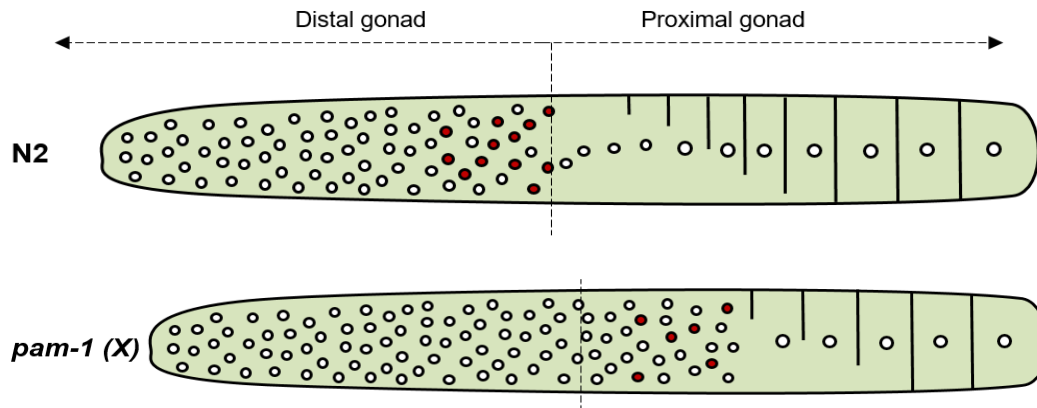


Figure 18: Model of pam-1 regulation of autophagy during gonadal culling. Above is the proposed mechanism by which autophagy is mediated by PAM-1 in the gonad. In wild type worms, PAM-1 is present to mediate nucleophagy in the proper location in the distal gonad. When pam-1 is mutated and the enzyme can no longer perform its function, gonadal culling by autophagy is not performed, and pachytene stage nuclei persist into the proximal gonad. Apoptotic culling is still present.

models, cells in the worm, including gonadal nuclei, were nutrient deficient. Autophagy is known to be stimulated in this environment. An upregulation of PAM-1 in collaboration with autophagic stimulation suggests further that the two processes are collaborating in the gonad.

In the RNAi models, however, there was also an upregulation of PAM-1 when autophagy genes were suppressed. In previous studies, *pam-1* influenced phenotypes trend away from wild-type when autophagy is suppressed using RNAi, but the trends are not statistically different. In the RNAi assays, PAM-1 was suspected to be upregulated due to the increasing brightness and timing of the GFP signal. This was surprising because PAM-1 upregulation was correlating a decrease in autophagic processes which appeared to contrast the starvation experiments and model of PAM-1 regulation of autophagic culling.

If PAM-1 was acting as a mediator of autophagy, one would predict the levels of PAM-1 to stay similar to normal state in an environment where autophagy proteins are suppressed, unless a feedback mechanism existed where a reduction in

autophagic vesicles or autophagic clearance led to an upregulation in autophagic mediators, such as PAM-1. This feedback mechanism would lead to a greater expression of PAM-1 in the nuclei, and likely a greater accumulation of PAM-1 perinuclearly, which is what was seen. This model could explain the limited impact of autophagy gene RNAi on wild-type worms in previous experiments (<10% suppression), as well as the drastic synergism that was seen when autophagy gene RNAi was done in a *pam-1* mutant background. Without the PAM-1 to collaborate with the autophagic response, a severe decrease in functional nurse cell nuclei degradation caused deficiencies in brood size, embryonic viability, and a notable expansion of pachytene stage nuclei.

The signaling mechanisms for PAM-1 activation and the potential feedback loop in this model are not as easily postulated. Signaling from the TOR pathway, as well as signals coming from specific nuclei that are to be degraded, could directly or indirectly increase PAM-1 levels in the cell and could also cause a perinuclear localization. PAM-1 could then act upon any number of targets in the perinuclear region to mediate autophagy. PAM-1 transcription could be shut off by a downstream signal of autophagy. In models where autophagy proteins are suppressed and autophagy functions are not complete, such as *bec-1* and *lgg-1* RNAi, the downstream signal will not shut down PAM-1 transcription, leading to higher levels of the protein in the nucleus. TOR signaling could continue to activate PAM-1 transcription and localization to the perinuclear region in models where starvation continues to impact the cell or when rapamycin is used to stimulate autophagy.

If the upregulation of PAM-1 has a direct effect on autophagic levels, PAM-1 may have a role in the formation of the PAS, a process that is not well understood. A mediation of PAS formation by PAM-1 could explain its perinuclear localization. Autophagosomes are normally made within the cell and trafficked to the membrane

by microtubules. In the syncytium of the worm gonad, trafficking to specific nuclei may be difficult. PAM-1 could mediate PAS formation close to the nuclear membrane as a mechanism of targeted nucleophagy. This could also be a mechanism for PAM-1 upregulation mediating an increase in autophagy. PAM-1 could recruit more PAS structures, thus increasing the number of autophagosomes and increasing autophagic clearance.

Perhaps the more likely mechanism of PAM-1 mediation of autophagy is through autophagosome localization (*Figure 19*). PSA has been known to have roles in membrane trafficking and has two microtubule binding domains (Constam *et al.*, 1995; Peer, 2011). PAM-1 is believed to target the microtubules during A-P

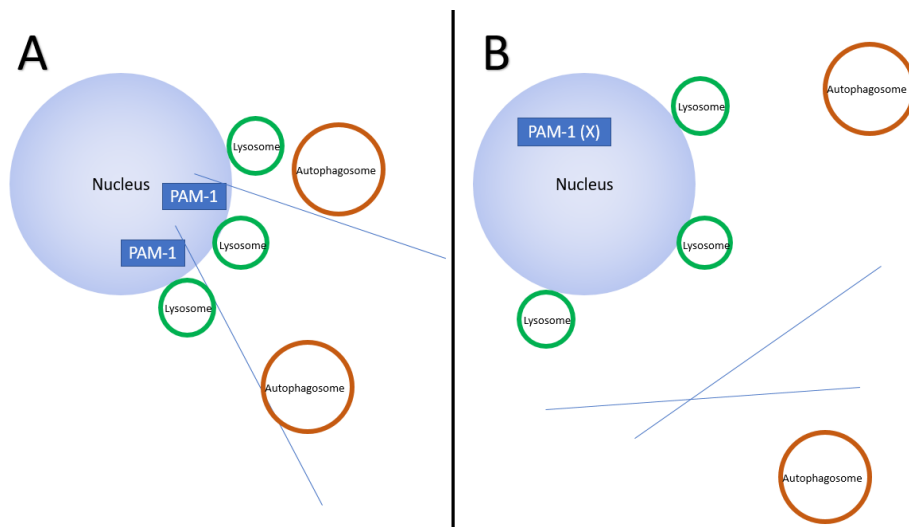


Figure 19: Potential mechanism of PAM-1 action. Above is a model of a proposed mechanism of PAM-1 function in regulating autophagy during gonadal culling. (A) In wild-type worms, PAM-1 binds microtubules that help localize autophagosomes to the nuclear membrane. The autophagosomes, once localized, will recognize the nucleus and degrade it. (B) When *pam-1* is mutant, it no longer binds microtubules. The microtubules are not localized to the nuclear membrane and autophagosomes encounter nuclei at a lower rate.

axis formation in embryonic development (Fortin *et al.*, 2010). As stated previously, autophagosomes are known to be delivered to the outer nuclear membrane by a microtubule network (Korolchuck *et al.*, 2001). PAM-1 may be functioning in localizing the autophagosomes to the nurse cell nuclei for

destruction. This mechanism of action could also explain the severity of *pam-1* mutant phenotypes; without PAM-1 functioning properly, it could not localize the autophagic structures for autophagy to take place at the rate required for proper development. Experimentation using microtubule and autophagosome markers could provide more detail about this potential interaction.

It is important to note that although PAM-1 is an aminopeptidase, a role within the lysosome as a degradative enzyme is unlikely. PAM-1 localizations within the nucleus make it a poor candidate for lysosomal action, as lysosomes accumulate perinuclearly outside the nucleus. In addition, a role of PAM-1 as a lysosomal enzyme would not explain the drastic effect of PAM-1 mutations on fecundity. The data we have thus far collected has argued against this potential mechanism.

In conclusion, data has been collected that suggests PAM-1 is likely to play a direct role in mediation of autophagy in the *C. elegans* gonad, but the mechanisms by which this occurs are unknown. These experiments align with previous data suggesting autophagy is likely a major component of nuclear culling in *C. elegans* oogenesis (Cude & Trzepacz, unpublished). Future experiments should focus on potential colocalizations of autophagic vesicles, as well as microtubules, to further elucidate the mechanism by which PAM-1 functions in autophagic culling. Characterizing and mutating a microtubule binding site in *pam-1* could assist in interpreting *pam-1* in this role.

The presented data's consistency with previous studies implicating *Psa*, the mammalian orthologue of *pam-1*, as an autophagic mediator suggests conservation of function across eukaryotic species and requires further investigation (Menzies *et al.*, 2010; Krupa *et al.*, 2013). These findings in *C. elegans* fertility could have implications in higher eukaryotic fertility. Autophagy may have similar roles in the destruction of nurse cells in *Drosophila melanogaster*, or could have evolved a

function in mammalian fertility. Further studies will need to be conducted to analyze these possibilities.

Works Cited

Abounit K, Scarabeli TM, McCauley RB. Autophagy in mammalian cells. *J Biol Chem* 2012; 3(1): 1-6.

Akematsu T, Pearlman RE, Endoh H. Gigantic macroautophagy in programmed nuclear death of *Tetrahymena thermophila*. *Autophagy* 2010; 6: 901-911.

Althoff MJ, Flick K, Trzepacz C. Collaboration within the M1 aminopeptidase family promotes reproductive success in *Caenorhabditis elegans*. *Dev Genes Evol* 2014; 224: 137-146.

Bence NF, Sampat RM, Kpito RR. Impairment of the ubiquitin-proteasome system by protein aggregation. *Science* 2001; 292: 1552-1555.

Bjorkoy G, Lamark T, Brech A, Outzen H, Perander M, Overvatn A, Stenmark H, Johansen T. p62/SQSTM1 forms protein aggregates degraded by autophagy and has a protective effect on huntingtin-induced cell death. *J Cell Bio* 2005; 171(4): 602-614.

Borsos E, Erdelyi P, Vellai T. Autophagy and apoptosis are redundantly required for *C. elegans* embryogenesis. *Autophagy* 2011; 7(5): 557-559.

Botbol V, Scornik OA. Peptide intermediates in the degradation of cellular proteins: Bestatin permits their accumulation in mouse liver *in vivo*. *J Biol Chem* 1983; 258: 1942-1949.

- Brenner S. The genetics of *Caenorhabditis elegans*. *Genetics* 1974; 77(1): 71-94.
- Brooks DR, Hooper NM, Isaac RE. The *Caenorhabditis elegans* orthologue of mammalian puromycin-sensitive aminopeptidase has roles in embryogenesis and reproduction. *J Biol Chem* 2003; 278(44): 42795-42801.
- Chen Y, Klionsky DJ. The regulation of autophagy – unanswered questions. *J Cell Sci* 2011; 124: 161-170.
- Choi AMK, Ryter SW, Levine B. Autophagy in human health and disease. *N Engl J Med* 2013; 368: 651-662.
- Chow KM, Guan H, Hersh LB. Aminopeptidases do not directly degrade tau protein. *Mol Neurodegener* 2010; 5: 48.
- Constam DB, Tobler AR, Rensing-Ehl A, Kemler I, Hersh LB, Fontana A. Puromycin-sensitive aminopeptidase. *J Biol Chem* 1995; 270(45): 26931-26939.
- Crichton D, Wilkinson S, O'Prey J, Syed N, Smith P, Harrison PR, Gasco M, Garrone O, Crook T, Ryan KM. DRAM, a p53-induced modulator of autophagy, is critical for apoptosis. *Cell* 2006; 126: 121-134.
- Cude A, Trzepacz C. PAM-1, the *C. elegans* ortholog of the puromycin sensitive aminopeptidase, collaborates with the autophagy pathway to promote fertility. Unpublished data.

- Daido S, Kanzawa T, Yamamoto A, Takeuchi H, Kondo Y, Kondo S. Pivotal role of the cell death factor BNIP3 in ceramide-induced autophagic cell death in malignant glioma cells. *Cancer Res* 2004; 62: 4286-4293
- Deter RL, De Duve C. Influence of glucagon, an inducer of cellular autophagy, on some physical properties of rat liver lysosomes. *J Cell Bio* 1967; 33: 437-449.
- Erdelyi P, Borsos E, Takacs-Vellai K, Kovacs T, Kovacs AL, Sigmond T, Hargitai B, Pasztor L, Sen Gupta T, Dengg M, Pesci I, Toth J, Nilsen H, Vertessy BG, Vellai T. Shared developmental roles and transcriptional control of autophagy and apoptosis in *Caenorhabditis elegans*. *J Cell Sci* 2010; 124: 1510-1518.
- Fazeli G, Trinkwalder M, Irmisch L, Wehman AM. C. elegans midbodies are released, phagocytosed, and undergo LC3-dependent degradation independent of macroautophagy. *J Cell Sci* 2016. 129(20): 3721-3731.
- Fortin S, Marshal SL, Jaeger EC, Greene PE, Brady LK, Isaac RE, Schrandt JC, Brooks DR, Lyczak R. The PAM-1 aminopeptidase regulates centrosome positioning to ensure anterior-posterior axis specification in one-cell *C. elegans* embryos. *Dev Bio* 2010; 334(2): 992-1000.
- Fraser AG, Kamath RS, Zipperlen P, Martinez-Campos M, Sohrmann M, Ahringer J. Functional genomic analysis of *C. elegans* chromosome I by systematic RNA interference. *Nature* 2000. 408(6810): 325-330.

- Gumienny TL, Lambie E, Harwig E, Horvitz RH, Hengartner MO. Genetic control of programmed cell death in the *Caenorhabditis elegans* hermaphrodite germline. *Development* 1999; 126: 1011-1022.
- He M, Kershaw MJ, Sones DM, Xia Y, Talbot NJ. Infection-associated nuclear degeneration in the rice blast fungus *Magnaporthe oryzae* requires non-selective macro-autophagy. *PLoS ONE* 2012; 7(3):e33270.
- Hersh LB, McKelvy JF. An Aminopeptidase from bovine brain which catalyzes the hydrolysis of enkephalin. *J Neurochem* 1981; 36(1): 171-178.
- Hubbard EJA, Greenstein D. The *Caenorhabditis elegans* gonad: a test tube for cell and developmental biology. *Dev Dynamics* 2000; 218: 2-22
- Hui KS, Wang RJ, Lajtha A. Purification and characterization of an enkephalin aminopeptidase from rat brain membranes. *Biochemistry* 1983; 22: 1062-1067.
- Itakura E, Mizushima N. Characterization of autophagosome formation site by a hierarchical analysis of mammalian Atg proteins. *Autophagy* 2010; 66: 764-776.
- Jahreiss L, Menzies FM, Rubinsztein DC. The itinerary of autophagosomes: from peripheral formation to kiss-and-run fusion with lysosomes. *Traffic* 2008; 9: 574-587,
- Kamath RS, Fraser AG, Dong Y, Poulin G, Durbin R, Gotta M, Kanapin A, Le Bot N, Moreno S, Sohrmann M, Welchman DP, Zipperlen P, Ahringer J.

Systematic functional analysis of the *Caenorhabditis elegans* genome using RNAi. *Nature* 2003; 421(6920): 231-237.

Kanazawa T, Taneike I, Akaishi R, Yoshizawa F, Furuya N, Fujimura S, Kadowaki M. Amino acids and insulin controls autophagic proteolysis through different signaling pathways in relation to mTOR in isolated rat hepatocytes. *J Biol Chem* 2004; 279: 8452-8459.

Kang R, Zeh HJ, Lotze MT, Tang D. The Beclin 1 network regulates autophagy and apoptosis. *Cell Death Differ* 2011; 18: 571-580.

Karsten SL, Sang TK, Gehman LT, Chatterjee S, Liu J, Lawless GM, Sengupta S, Berry RW, Pomakian J, Oh HS, Schulz C, Jui KS, Wiedau-Pazos M, Vinters HV, Binder LI, Geschwind DH, Jackson GR. A genomic screen for modifiers of tauopathy identifies Puromycin-sensitive aminopeptidase as an inhibitor of Tau-induced neurodegeneration. *Neuron* 2006; 51: 549-560.

Kim J, Haung WP, Klionsky DJ. Membrane recruitment of Aut7p in the autophagy and cytoplasm to vacuole targeting pathways requires Aut1p, Aut2p and autophagy conjugation complex. *J Cell Biol* 2001; 152: 51-64.

Kita H, Carmichael J, Swartz J, Muro S, Wytenbach A, Matsubara K, Rubinsztein DC, Kato K. Modulation of polyglutamine-induced cell death by genes identified by expression profiling. *Hum Mol Genet* 2002; 11: 2279-2287.

- Klionsky DJ, Cregg JM, Dunn WA Jr, Emr SD, Sakai Y, Sandoval IV, Sibirny A, Subramani S, Thumm M, Veenhuis M, Ohsumi Y. A unified nomenclature for yeast Autophagy-related genes. *Dev Cell* 2003; 5: 539-545.
- Komatsu M, Waguri S, Kolike M, Sou YS, Ueno T, Hara T, Mizushima N, Iwata JI, Ezaki J, Murata S *et al.* Homeostatic levels of p62 control cytoplasmic inclusion body formation in autophagy-deficient mice. *Cell* 2007; 131: 1149-1163.
- Korolchuk VIK, Rubinsztein DC. Regulation of autophagy by lysosomal positioning. *Autophagy* 2011; 7(8): 927-928.
- Korolchuk VI, Saiki S, Maiké L, Siddiqi FH, Roberts EA, Imarisio S, Jahreiss L, Sarkar S, Futter M, Menzies FM, O’Kane CJ, Deretic V, Rubinsztein DC. Lysosomal Positioning coordinates cellular nutrient responses. *Nat Cell Biol* 2001; 13(4): 453-460.
- Krupa AJ, Ott S, Chandraratna DS, Irving JA, Page RM, Speretta E, Seto T, Camargo LM, Marciniak SJ, Lomas DA, Crowther DC. Suppression of A β toxicity by puromycin-sensitive aminopeptidase is independent of its proteolytic activity. *Biochimica et Biophysica Acta* 2013; 1832: 2115-2126.
- Kudo LC, Parfenova L, Ren G, Vi N, Hui M, Ma Z, Lau K, Gray M, Bardag-Gorce F, Wiedau-Pazos M, Hui KS, Karsten SL. Puromycin-sensitive aminopeptidase (PSA/NPEPPS) impedes development of neuropathology

in hPSA/TAU^{P301L} double-transgenic mice. *Hum Mol Gen* 2011; 20(9): 1820-1833.

Lendeckel U, Arndt M, Frank K, Spiess A, Reinhold D, Ansorge S. Modulation of WNT-5A expression by actinonin: linkage of APN to the WNT-pathway? *Adv Exp Med Biol* 2000; 477: 35-41.

Liang XH, Kleeman LK, Jiang HH, Gordon G, Goldman JE, Berry G, Herman B, Levine B. Protection against fatal sindbis virus encephalitis by Beclin, a novel Bcl-2-interacting protein. *J Virol* 1998; 72: 8586-8596.

Lum JJ, DeBerardinis RJ, Thompson CB. Autophagy in metazoans: cell survival in the land of the plenty. *Nat Rev* 2005; 6: 439-448.

Lyczak R, Zweier L, Group T, Murrow MA, Snyder C, Kulovitz L, Beatty A, Smith K, Bowerman B. The puromycin-sensitive aminopeptidase PAM-1 is required for meiotic exit and anteroposterior polarity in the one-cell *Caenorhabditis elegans* embryo. *Development* 2006; 133: 4281-4292.

Mijaljica D, Devenish RJ. Nucleophagy at a glance. *J Cell Sci* 2013; 126: 4325-4330.

Massey A, Kiffin R, Cuervo AM. Pathophysiology of chaperone-mediated autophagy. *Int J Biochem Cell Biol* 2004; 36: 2420-2434.

Mehrpour M, Esclatine A, Beau I, Codogno P. Autophagy in health and disease. 1. Regulation and significance of autophagy: an overview. *Am J Physiol Cell Physiol* 2010; 298: C776-C785.

- Meley D, Bauvy C, Houben-Weerts JH, Dubbelhuis PF, Helmond MT, Codogno P, Meijer AJ. AMP-activated protein kinase and the regulation of autophagic proteolysis. *J Biol Chem* 2006; 281 1387-1391.
- Menzies FM, Hourez R, Imarisio S, Raspe M, Sadiq O, Chandaratna D, Kane CO, Rock KL, Reits E, Goldberg AL, Rubinsztein DC. Puromycin-sensitive aminopeptidase protects against aggregation-prone proteins via autophagy. *Hum Mol Gen* 2010; 19(23): 4573-4586.
- Mills KR, Reginato M, Debnath J, Queenan B, Brugge JS. Tumor necrosis factor-related apoptosis-inducing ligand (TRAIL) is required for induction of autophagy during lumen formation in vitro. *Proc Natl Acad Sci* 2004; 101: 3438-3443.
- Mizushima N. Autophagy: process and function. *Genes Dev* 2007; 21: 2861-2873.
- Mizushima N, Komatsu M. Autophagy: renovation of cells and tissues. *Cell* 2011; 147: 728-741.
- Mochida K, Oikawa Y, Kimura Y, Kirisako H, Hirano H, Ohsumi Y, Nakatogawa H. Receptor-mediated selective autophagy degrades the endoplasmic reticulum and the nucleus. *Nature* 2015; 522: 359-362.
- Mordier S, Deval C, Bechet D, Tassa A, Ferrara M. Leucine limitation induces autophagy and activation of lysosome-dependent proteolysis in C2C12 myotubes through a mammalian target of rapamycin-independent signaling pathway. *J Biol Chem* 2000; 275: 29900-29906.

- Mortimore GE, Poso AR. Intracellular protein catabolism and its control during nutrient deprivation and supply. *Ann Rev Nutr* 1987; 7: 539-564.
- Nakatogawa H, Suzuki K, Kamada Y, Ohsumi Y. Dynamics and diversity in autophagy mechanisms: lessons from yeast. *Nat Rev* 2009; 10: 458-467.
- Nakatogawa H. Eating the ER and the nucleus for survival under starvation conditions. *Mol Cell Oncol* 2016; 3(2): e1073416.
- Okamoto K. Organellophagy: eliminating cellular building blocks via selective autophagy. *J Cell Biol* 2014; 205: 435-445.
- Osada T, Ikegami S, Takiguchi-Hayashi K, Yamazaki Y, Katohfukui Y, Higashinakagawa T, Sakaki Y, Takeuchi T. Increased anxiety and impaired pain response in puromycin-sensitive aminopeptidase gene-deficient mice obtained by a mouse gene-trap method. *J Neurosci* 1999; 19: 6068-6078.
- Osada T, Watanabe G, Kondo S, Toyoda M, Sakaki Y, Takeuchi T. Male reproductive defects caused by puromycin-sensitive aminopeptidase deficiency in mice. *Mol Endo* 2001a; 15: 960-971.
- Osada Watanabe G, Sakaki Y, Takeuchi T. Puromycin-sensitive aminopeptidase is essential for the maternal recognition of pregnancy in mice. *Mol Endo* 2001b; 15: 882-893.
- Pang KM, Ishidate T, Nakamura K, Shirayama M, Trzepacz C, Schubert CM, Priess JR, Mello CC. The minibrain kinase homolog mbk-2, is required for

spindle positioning and asymmetric cell division in early *C. elegans* embryos. *Dev Biol* 2004; 265(1): 127-139.

Park YE, Hayashi YK, Bonne G, Arimura T, Noguchi S, Nonaka I, Nishino I. Autophagic degradation of nuclear components in mammalian cells. *Autophagy* 2009; 5(6): 795-804.

Peer WA. The role of multifunctional M1 metallopeptidases in cell cycle progression. *Ann Bot* 2011; 107(7): 1171-1181.

Pickrell AM, Youle RJ. The roles in PINK1, parkin and mitochondrial fidelity in Parkinson disease. *Neuron* 2015; 85: 257-273.

Pino EC, Webster CM, Carr CE, Soukas AA. Biochemical and high throughput microscopic assessment of fat mass in *Caenorhabditis elegans*. *J Vis Exp* 2013; 73: e50180.

Pyo JO, Jang MH, Kwon YK, Lee HJ, Jun JI, Woo HN, Cho DH, Choi B, Lee H, Kim JH, Mizushima N, Oshumi Y, Jung YK. Essential roles of Atg5 and FADD in autophagic cell death: dissection of autophagic cell death into vacuole formation and cell death. *J Biol Chem* 2005; 280: 20722-20729.

Reef S, Zalckvar E, Shifman O, Bialik S, Sabanay H, Oren M, Kimchi A. A short mitochondrial form of p19ARF induced autophagy and caspas-independent cell death. *Mol Cell* 2006; 22: 463-475.

Ren G, Ma Z, Hui M, Kudo LC, Hui KS, Karsten SL. Cu, Zn-superoxide dismutase 1 (SOD1) is a novel target of Puromycin-sensitive aminopeptidase

(PSA/NPEPPS): PSA/NPEPPS is a possible modifier of amyotrophic lateral sclerosis. *Mol Neurodegener* 2011; 6: 29.

Saric T, Beninga J, Graef CI, Akopian TN, Rock KL, Goldberg AL. Major histocompatibility complex class I-presented antigenic peptides are degraded in cytosolic extracts primarily by thimet oligopeptidase. *J Biol Chem* 2001; 276: 36474-36481.

Sarkar S, Perlstein EO, Imarisio S, Pineau S, Cordenier A, Maglathlin RL, Webster JA, Lewis TA, O'Kane CJ, Schreiber SL. Small molecules enhance autophagy and reduce toxicity in Huntington's disease models. *Nat Chem Biol* 2007; 3: 331-338.

Sato M, Sato K. Degradation of paternal mitochondria by fertilization-triggered autophagy in *C. elegans* embryos. *Science* 2011; 334: 1141-1144.

Schedl T. Developmental genetics of the germ line in *C. elegans II*. (ed. DL Riddle, T Blumenthal, BJ Meyer, JR Priess). 1997. Pp. 241-270. Plainview: Cold Spring Harbor Laboratory Press.

Schiavi A, Torgovnick A, Kell A, Megalou E, Castelein N, Guccini I, Marzocchella L, Gelino S, Hansen M, Malisan F, Condo' I, Bei R, Rea S, Braeckman BP, Tavernarakis N, Testi R, Ventura N. Autophagy induction extends lifespan and reduces lipid content in response to frataxin silencing in *C. elegans*. *Exp Gerontol* 2013; 48: 191-201.

- Schulz C, Perezgasga L, Fuller MT. Genetic analysis of *dPsa*, the *Drosophila* orthologue of puromycin-sensitive aminopeptidase, suggests redundancy of aminopeptidases. *Dev Genes Evol* 2001; 211: 581-588.
- Shoji JY, Kikuma T, Arioka M, Kitamoto K. Macroautophagy-mediated degradation of whole nuclei in the filamentous fungus *Aspergillus oryzae*. *PLoS ONE* 2010; 5: e15650.
- Shpilka T, Weidberg H, Pietrokovski S, Elazar Z. Atg8: an autophagy-related ubiquitin-like protein family. *Gen Biol* 2011; 12: 226.
- Stoltze L, Schirle M, Schwarz G, Schroter C, Thompson MW, Hersch LB, Kalbacher H, Stebanovic S, Rammensee HG, Schild H. Two new proteases in the MHC class I processing pathway. *Nat Immunol* 2000; 1: 413-418.
- Suzuki K, Ohsumi Y. Molecular machinery of autophagosomes formation in yeast, *Saccharomyces cerevisiae*. *FEBS Lett* 2007; 581: 2156-2161.
- Suzuki K, Kirisako T, Kamada Y, Mizushima N, Noda T, Ohsumi Y. The pre-autophagosomal structure organized by concerted functions of *APG* genes is essential for autophagosome formation. *EMBO J* 2001; 20: 5971-5981.
- Takacs-Vellai K, Vellai T, Puoti A, Passannante M, Wicky C, Streit A, Kovacs AL, Muller F. Inactivation of the autophagy gene *bec-1* triggers apoptotic cell death in *C. elegans*. *Current Biology* 2005; 15: 1513-1517.

- Takeshige K, Baba M, Tsuboi S, Noda T, Ohsumi Y. Autophagy in yeast demonstrated with proteinase-deficient mutants and conditions for its induction. *J Cell Biol* 1992; 119(2): 301-311.
- Tasdemir E, Galluzzi L, Maiuri MC, Criollo A, Vitale I, Hangen E, Modjtahedi N, Kroemer G. Methods for assessing autophagy and autophagic cell death. *Methods Mol Biol* 2008; 445: 29-76.
- Taylor A. Aminopeptidases: towards a mechanism of action. *Trends Biochem Sci* 1993; 18: 167-171.
- Thorburn J, Moore F, Rao A, Barclay WW, Thomas LR, Grant KW, Cramer SD, Thorburn A. Selective inactivation of a Fas-associated death domain protein (FADD)-dependent apoptosis and autophagy pathway in immortal epithelial cells. *Mol Biol Cell* 2005; 16: 1189-1199.
- Timmons L, Court DL, Fire A. Ingestion of bacterially expressed dsRNA's can produce specific and potent genetic interference in *Caenorhabditis elegans*. *Gene* 2001; 263(1-2): 103-112.
- Timmons L, Fire A. Specific interference by ingested dsRNA. *Nature* 1998; 395: 854.
- Tokunaga C, Yoshino K, Yonezawa K. mTOR integrates amino acid- and energy-sensing pathways. *Biochem Biophys Res Commun* 2004; 313: 443-446.
- Towne CF, York IA, Neijssen J, Karow ML, Murphy AJ, Valenzuela DM, Yancopoulos GD, Neefjes JJ, Rock KL. Puromycin-sensitive

aminopeptidase limits MHC class I presentation in dendritic cells but does not affect CD8 T cell responses during viral infections. *J Immunol* 2008; 180: 1704-1712.

Trinkwalder M, Irmisch L, Wehman AM. *C. elegans* midbodies are released, phagocytosed, and undergo LC3-dependent degradation independent of macroautophagy. *J Cell Sci* 2016; 129(20): 3721-3731.

Yang Z, Huang J, Geng J, Nair U, Klionsky DJ. Atg 22 recycles amino acids to link the degradative and recycling functions of autophagy. *Mol Biol Cell* 2006; 17: 5094-5104.

Yang Z, Klionsky DJ. An overview of the molecular mechanism of autophagy. *Curr Top Microbiol Immunol* 2009; 335: 1-32.

Yao T, Cohen RE. Giant proteases: beyond the proteasome. *Curr Biol* 1999; 9: R551-R553.